

# **The Mobile VR-Amblyopia Trainer. An Android Based VR-Game for the Treatment of Amblyopia.**

## **Bachelor's Thesis in Medical Engineering**

submitted  
by

Antonia Steger

born 16.11.1998 in Bad Mergentheim

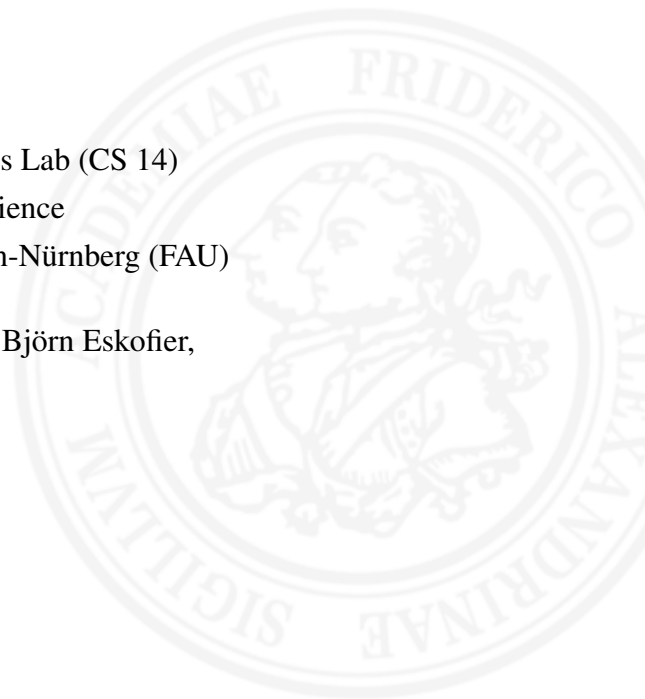
Written at

Machine Learning and Data Analytics Lab (CS 14)  
Department of Computer Science  
Friedrich-Alexander-Universität Erlangen-Nürnberg (FAU)

Advisors: Wolfgang Mehringer, Markus Wirth, Prof. Dr. Björn Eskofier,  
Prof. Dr. Georg Michelson

Started: 31.08.2020

Finished: 11.02.2021





Ich versichere, dass ich die Arbeit ohne fremde Hilfe und ohne Benutzung anderer als der angegebenen Quellen angefertigt habe und dass die Arbeit in gleicher oder ähnlicher Form noch keiner anderen Prüfungsbehörde vorgelegen hat und von dieser als Teil einer Prüfungsleistung angenommen wurde. Alle Ausführungen, die wörtlich oder sinngemäß übernommen wurden, sind als solche gekennzeichnet.

Die Richtlinien des Lehrstuhls für Bachelor- und Masterarbeiten habe ich gelesen und anerkannt, insbesondere die Regelung des Nutzungsrechts.

Erlangen, den 11. Februar 2021



## Übersicht

Etwa 1,3 % bis 3,6 % aller Kinder leiden an Amblyopie, einer Fehlfunktion des visuellen Systems, die durch Vorerkrankungen wie Strabismus (Schielen) und Anisometropie (unterschiedliche Brechkraft beider Augen) verursacht wird. Aufgrund der Vorerkrankungen sieht das amblyope Auge wesentlich schlechter als das Andere, weshalb das Gehirn die Informationen des schlechteren Auges unterdrückt. Unbehandelt kann die Krankheit zu lebenslangen Problemen des visuellen Systems führen. Die häufigste Form der Therapie ist das Patching, wobei das amblyope Auge unter monokularen Bedingungen trainiert wird. Die monokulare Therapie birgt jedoch Nachteile wie die Verschlechterung der Sehschärfe des gesunden Auges. Neuere Therapieansätze arbeiten deshalb binokular. Das bedeutet, dass beide Augen zusammen arbeiten wodurch ihre Tiefenwahrnehmung trainiert und die Sehschärfe des amblyopen Auges verbessert werden kann.

In dieser Arbeit wird eine binokulare Therapie in Form eines Virtual Reality Spiels eingesetzt. Die Anwendung ist in der Lage, Strabismus und Anisometropie so zu kompensieren, dass die von beiden Augen empfangenen Bildqualitäten angeglichen werden. Dies begünstigt die Beseitigung der Unterdrückung des amblyopen Auges. Ziel der Arbeit ist es, den sogenannten VR-Amblyopia Trainer so zu modifizieren, dass er auf einem Standalone-Gerät, der Vive Focus Plus, funktioniert, um eine regelmäßige und unabhängige Therapie zu Hause zu ermöglichen. Aus diesem Grund musste die Anwendung in ihrer Komplexität reduziert werden und die Rendering-Einstellungen an die geringere Rechenleistung der Vive Focus Plus angepasst werden. Um den VR-Amblyopia Trainer auf beiden Geräten zu vergleichen, wurde eine Studie durchgeführt, in der 20 gesunde Probanden im Alter von  $22,65 \pm 1,88$  Jahren beide Geräte im Abstand von genau sieben Tagen testeten. Nach beiden Durchläufen wurden zwei Fragebögen zur Benutzerfreundlichkeit und zum Präsenzepfinden beantwortet.

Besonders starke Signifikanzen ( $p < 0.01$ ) treten im Stereopsis Level auf. Darin sind die mittleren Reaktionszeiten des Standalone-Gerätes im Schnitt 43,5 ms größer. Bei der Schielwinkelmessung treten nur vereinzelt leichte ( $p < 0.05$ ) und mittlere ( $p < 0.01$ ) Signifikanzen auf, wobei das Standalone-Gerät betragsweise größere Verschiebungen misst. Lediglich im Suppressions Level sind die Ergebnisse beider Geräte ohne Signifikanzen. Abweichende Ergebnisse der Schielwinkelmessung könnten darauf zurückzuführen sein, dass die Bildqualität des Standalone-Gerätes reduziert wurde um dadurch den Rechenaufwand zu verringern. Die starken Signifikanzen im Stereopsis Level weisen jedoch darauf hin, dass das Spielgeschehen für die geringere Rechenleistung zu dynamisch ist. Da mit dem Suppressions Level allerdings bewiesen wurde, dass es auf dem Standalone-Gerät möglich ist gute Ergebnisse zu erreichen, sollten zukünftige Arbeiten darauf abzielen, die Komplexität des Stereopsis Levels weiter zu reduzieren.

## Abstract

About 1.3 % to 3.6 % of all children suffer from amblyopia, a disorder of the visual system caused by previous diseases such as strabismus (squinting) and anisometropia (different refractive power of both eyes). Due to these previous diseases, the amblyopic eye sees worse than the other one, which is why the brain suppresses the information from this eye. If left untreated, the disease can lead to lifelong problems of the visual system. The most common form of therapy is patching, which involves training the amblyopic eye under monocular conditions. However, monocular therapy has disadvantages such as the deterioration of the visual acuity of the healthy eye. For this reason, more recent therapy approaches work binocularly, which means that both eyes train together and thus improve their depth perception and the visual acuity of the amblyopic eye.

In this work, a binocular therapy in the form of a Virtual Reality game is used. The application can compensate for strabismus and anisometropia in such a way that the image qualities received by both eyes are aligned, thus supporting the removal of the suppression of the amblyopic eye. The goal of this thesis is to modify the so-called VR-Amblyopia Trainer in a way that it works on a standalone device, the Vive Focus Plus, in order to enable regular and independent therapy at home. For this reason, the application had to be reduced in complexity and the rendering settings had to be adjusted to match the lower computing power of the Vive Focus Plus. To compare the VR-Amblyopia Trainer on both devices, a study was conducted, in which 20 healthy subjects aged  $22.65 \pm 1.88$  years tested both devices exactly seven days apart. After both runs, two questionnaires on usability and sense of presence were answered.

Particularly strong significances ( $p < 0.01$ ) occur in the stereopsis level. At this level, the mean reaction times of the standalone device are on average 43.5 ms larger. In the squint angle measurement only small ( $p < 0.05$ ) and medium ( $p < 0.01$ ) significances occur, whereby the standalone device measures larger shifts. Only at the suppression level are the results of both devices without significances. Deviating results of the squint angle measurement could be due to the fact that the image quality of the standalone device was reduced in order to reduce the computational effort. The strong significances in the stereopsis level, on the other hand, indicate that the gameplay is too dynamic for the lower computational power. However, since the suppression level has proven that it is possible to achieve good results on the standalone device, future work should aim to further reduce the complexity of the stereopsis level.

# Contents

<b>1</b>	<b>Introduction</b>	<b>1</b>
<b>2</b>	<b>Fundamentals</b>	<b>3</b>
2.1	Structure of the Eye . . . . .	3
2.2	Binocular and Stereoscopic Vision . . . . .	4
2.3	Disorders of the Visual System . . . . .	6
2.3.1	Strabismus . . . . .	6
2.3.2	Refraction Error and Anisometropia . . . . .	7
2.3.3	Amblyopia . . . . .	9
2.3.4	Treatment of Amblyopia . . . . .	9
<b>3</b>	<b>Related Work</b>	<b>13</b>
3.1	Monocular Treatment . . . . .	13
3.2	Binocular Treatment . . . . .	15
<b>4</b>	<b>Methods</b>	<b>19</b>
4.1	HTC Vive Pro and HTC Vive Focus Plus . . . . .	19
4.2	VR-Amblyopia Trainer . . . . .	20
4.2.1	Strabismus Measurement . . . . .	22
4.2.2	Suppression Measurement . . . . .	24
4.2.3	Stereopsis Level . . . . .	26
4.3	Modification for the Standalone Device . . . . .	28
4.4	User Study . . . . .	30
4.4.1	Participants . . . . .	30
4.4.2	Procedure . . . . .	31
4.5	Data Processing . . . . .	33

<b>5</b>	<b>Results</b>	<b>35</b>
5.1	Visual Acuity . . . . .	35
5.2	VR-Amblyopia Trainer Results . . . . .	36
5.2.1	Strabismus Level . . . . .	36
5.2.2	Suppression Level . . . . .	39
5.2.3	Stereopsis Level . . . . .	40
5.3	SuS and IPQ . . . . .	41
<b>6</b>	<b>Discussion</b>	<b>45</b>
6.1	Visual Acuity . . . . .	45
6.2	Strabismus Level . . . . .	46
6.3	Suppression Level . . . . .	48
6.4	Stereopsis Level . . . . .	48
6.5	SuS and IPQ . . . . .	50
<b>7</b>	<b>Conclusion and Future Work</b>	<b>53</b>
<b>A</b>	<b>Patents</b>	<b>55</b>
A.1	Method and apparatus for the treatment of amblyopia . . . . .	55
A.2	Interactive system for vision assesment and correction . . . . .	56
A.3	Method and apparatus for treating diplopia and convergence insufficiency disorder	57
	<b>List of Figures</b>	<b>58</b>
	<b>List of Tables</b>	<b>62</b>
	<b>Bibliography</b>	<b>64</b>



# Chapter 1

## Introduction

Amblyopia is a disease of the visual system, which often leads to a reduction in visual acuity in the affected eye [Hol06]. One cause of amblyopia is strabismus, a malfunction in which the movement of the eyes is not symmetrical, hence, they cannot focus on the same point [Hol06, Lev06]. The disease often arises in early childhood and should be diagnosed and treated as soon as possible to avoid a lifelong visual impairment [Hol11]. The common treatment over the last decades for amblyopia in children was and still is patching. The healthy eye is covered with a patch so that the brain is forced to process the information from the amblyopic eye [Sea00]. However, the therapy has disadvantages [Hes15]. First, there are psychological issues especially for children: On the one hand they are restricted in their activities because of the reduced visual performance. On the other hand young children tend to not understand why the healthy eye is covered and they are forced to use the amblyopic eye [Sea00, Hes15]. Secondly, it has medical disadvantages: While patching improves visual acuity, it reduces the ability of depth perception. This is because patients are only allowed to use one eye while the other is patched [Hol06]. With the advent of Virtual Reality (VR) technology new possibilities arise to the treatment of amblyopia in which both eyes are used simultaneously, also called binocular treatment [Fos17]. The advantage of binocular treatment in VR is the ability to show distinct images to each eye. In this way, it is possible to equalize the image quality of the non-amblyopic eye. Thus, the brain accepts both visual inputs and both eyes are forced to work together [Eas06]. This can directly train the binocular performance. Regularly applied to an amblyope can help to cure the visual disease.

Such a binocular treatment is already realized as VR game and parts of the game are published [Meh20]. This game consists of three parts: First the strabismus measurement to compensate any misalignments, second the suppression measurement to equalize the image quality of both eyes and enable binocular vision, and third the stereopsis level which trains stereoacuity with defined

disparity settings. However, the application is currently solely available for a wired VR headset, the HTC Vive Pro. This device is operated by a high-performance computer and additionally requires a permanently installed tracking system to allow the headset to determine its position in the room. This complex hardware setup increases the costs for the game and introduces the risk of user errors. Additionally, it is inflexible in its use due to the permanently installed tracking system that has to be recalibrated when relocated. These additional hardware components complicate a periodic usage at home which is important for a successful therapy of amblyopia.

The goal of this thesis is to modify the implemented binocular treatment in a way that it can be used on standalone VR devices. The advantage of these VR devices is that only headset and controllers are needed. The headset locates itself in the room and the controllers are tracked relative to the headset. This minimizes the effect of the above mentioned disadvantages, because the device is reduced in costs and can easily be used at home and by the patient. The ease of use due to less hardware makes the system particularly suitable for therapy at home, as the system can be easily transported and used in different locations quickly and easily.

# Chapter 2

## Fundamentals

The visual system is the basis of one of the most important human senses, the sense of sight. It enables the visual perception of the environment by processing large amounts of information very quickly. Through visual information, humans are not only able to determine where objects are located [Atc00]. It is also possible to estimate the distance between several objects and their size. This enables the improvement of fine motor skills by adjusting the finger alignment and the orientation of hands before grabbing an object [Wat04]. This chapter deals with the basic process of image perception in the human eye and the function of binocular vision. Furthermore, it describes the diseases of strabismus, refraction error and amblyopia that affect the quality of vision.

### 2.1 Structure of the Eye

The human eye is a very complex organ with many different components that contribute to the ability of humans to perceive their environment. Figure 2.1 illustrates the basic elements of the eye, whose properties and influence on the perception of sharp images are described below.

The imaging process begins with light entering the eye through the cornea and the pupil. The amount of light that comes into the eye can be adapted to the lighting conditions by adjusting the pupil size. After the light has crossed the lens and the inside of the vitreous body, it hits the retina. The retina is located opposite the lens on the inside of the vitreous body, where it covers the surface as a skin. The actual image perception in the human eye takes place at the retina. It is an extension of the central nervous system and consists of light-sensitive cells that convert the incoming light into electrical impulses and transmit them to the brain via the optic nerve [Atc00].

To ensure that the surroundings can be perceived as a sharp image, the incident light must be

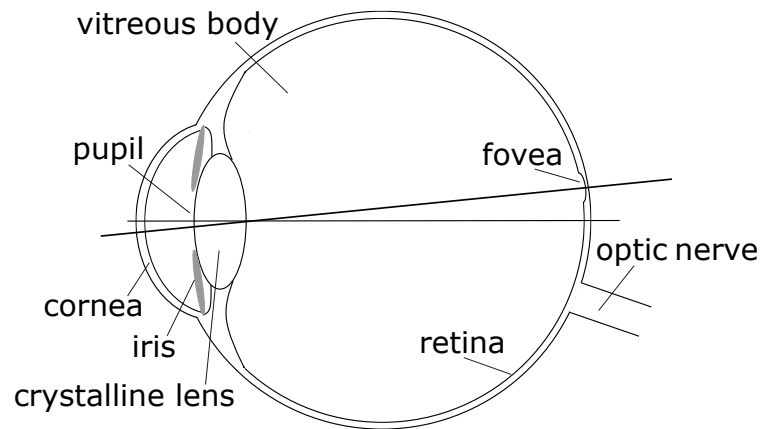


Figure 2.1: **Structure of the human eye.** The anatomy of the human eye, including the elements mentioned in chapter 2.1, based on [Atc00].

focused on the retina. Therefore, the light is initially refracted at the cornea and the lens. The cornea has the stronger refractive power of both, but the refraction cannot be changed since there are no muscles attached to the cornea. The curvature of the lens, however, can be adjusted to such an amount that objects at different distances can be exactly imaged on the retina, when they are targeted. This adjustment of refraction is called accommodation, whereby the shape of the lens is changed to the corresponding shape using the muscles attached to it. The spot of greatest visual acuity on the retina is called the fovea, which is why every object fixed by the eyes is mapped on it [Atc00].

## 2.2 Binocular and Stereoscopic Vision

Binocular vision describes the fact that the environment is seen through two eyes. They enlarge the field of view and improve contrast sensitivity and visual acuity. In humans, the eyes are placed on each side of the nose, which results in a certain pupillary distance. This anatomy allows two slightly different images of the surroundings to be perceived, but the field of view still overlaps. This overlap is called binocular overlap [Atc00]. Besides the shifted field of view of both eyes, the retinal images differ in the area of binocular overlap in a way that both eyes look at three-dimensional objects from two different perspectives [How95]. Because of these different

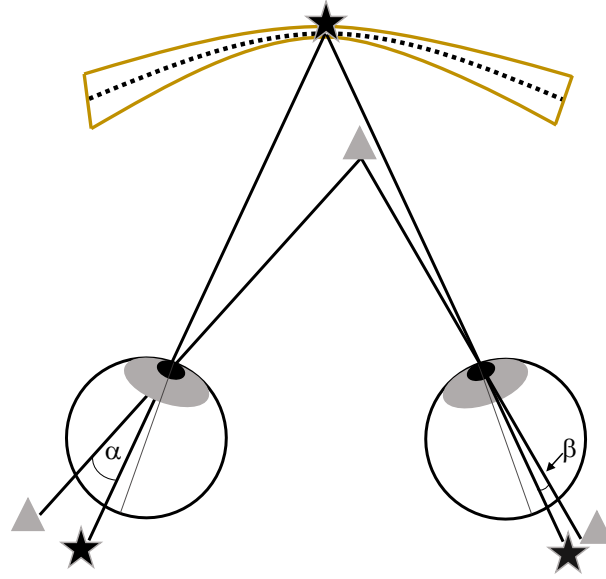


Figure 2.2: **Stereopsis in human eyes.** The star is focused with both eyes, whereby being imaged on the fovea. Due to the alignment of the eyes, the triangle falls with two different angles  $\alpha$  and  $\beta$  through the eyes at two non-corresponding points on the retinas. The distance between the triangle and the star can be calculated with the help of the projection points. Additionally, the dashed line illustrates the Empirical Horopter, which runs through the focused star. The yellow lines represent the boundaries of the Panum's fusional area. Based on [Nit17, Wri06].

perspectives, it is possible for humans to receive 3D information, even though the environment is displayed on a 2D retina [Nit17].

In order to get depth information, the monocular images of both eyes are fused into one binocular image. Particular attention is paid to projection points, that describe the position at which an object is imaged on the retina. In eyes without strabismus, focused objects are always projected on the foveas, which are located at the same place on both retinas and are therefore called corresponding retinal points. Corresponding retinal points are always points that are located at the same place on both retinas. Through the fixed object runs an imaginary elliptical line called Empirical Horopter. All points on this line are projected onto corresponding retinal points as well. In Figure 2.2 the star is targeted and mapped to the foveas accordingly and the dashed line represents the Empirical Horopter [Wri06].

However, humans are only able to focus on one single object at a time. For this reason and because of the offset position of the eyes, all objects in front of and behind the Empirical Horopter are mapped to non-corresponding points of each retina [Wri06]. This is illustrated in Figure 2.2 with a triangle, which is located in front of the Empirical Horopter. While the eyes are aligned to

focus on the star, the triangle falls through the lens onto the retina from a different angle  $\alpha$  and  $\beta$  in both eyes. This means that the projection points of the triangle are at different distances from the foveas in both eyes. This distance is called binocular disparity and is calculated by the difference of  $\alpha$  and  $\beta$ . Due to these disparities, the brain is able to recognize whether an object is in front of or behind the fixed object [Nit17]. This ability of depth perception is also called stereopsis or stereoscopic vision [How95]. In addition, the disparities cause the fused images to appear blurred or as double images in the peripheral area. This is due to the fact that during fusion both retinal images are superimposed over each other. And thus, in places where different objects were imaged on corresponding retinal points, different objects are superimposed. However, there is a finite area in front of and behind the empirical horopter, called Panum's fusional area. All objects in this area are fused into one image, although they are imaged on slightly non-corresponding retinal points. The Panum's fusional area is also illustrated in Figure 2.2 [Wri06].

## 2.3 Disorders of the Visual System

Due to errors in the anatomy of the eyes or faulty cooperation of the various components needed for image perception, the visual system may not be able to transmit optimal images to the brain. This chapter describes the causes and effects of the disorders strabismus, refraction error and amblyopia.

### 2.3.1 Strabismus

The decisive starting point for successful binocular vision in humans is the ability to align both eyes in such a way that they both image a fixed object exactly on the fovea [Eco12]. The control of the extraocular muscles is crucial for this. They must be able to hold the eyes in one position during fixation as well as move both eyes symmetrically in all directions [Sin12]. This correct cooperation of the extraocular muscles develops in the first years of life. In about 2 % of children, this development is impeded which disturbs the correct coordination of both eyes [Eco12]. One resulting defective eye movement is called strabismus. It is a disease of the visual system in which the movement of the eyes is not symmetrical, hence, they cannot focus on the same point. If it is not possible to focus both eyes on the same target, two different objects are imaged on the two foveas, shown in Figure 2.3. As a result, the brain is no longer able to fuse the two retinal images, because different objects are projected onto corresponding points [Bui14]. To avoid the issue of double vision, the brain of strabismus patients suppresses the information from the squinting eye. As a consequence, they have a sharp view of the surroundings, but since the squinting eye is no

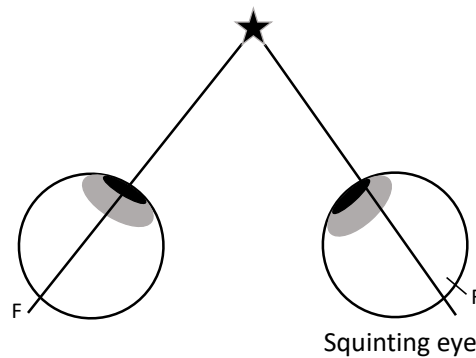


Figure 2.3: **Strabismus.** While the left eye focuses on the star, which is accordingly imaged on its fovea (F), the squinting eye is not aligned accordingly and the star is imaged on a non-corresponding point, based on [Wri06].

longer used, it cannot perform its functions, which gradually causes it to atrophy and its visual acuity to deteriorate [Eco12].

Strabismus can be divided into latent and manifest strabismus. Latent strabismus often remains undetected because both eyes are able to simultaneously target the same object. The squinting eye will only deviate from the actual direction if the binocular vision is interrupted. However, such an interruption normally only occurs if it is artificially induced by simply covering one of the eyes or by showing different images to both eyes. Therefore latent squint has no influence on binocular vision because the brain is still able to merge the information from both eyes. Since binocular vision is not interrupted in normal everyday life, it often happens that those affected are unaware of their latent strabismus. The manifest strabismus, on the other hand, is always recognizable. The eyes are not able to move symmetrically or point and focus on the same object simultaneously. Consequently, manifest strabismus leads to double vision, which the brain, in turn, tries to prevent by suppression of the squinting eye. For this reason, this type of strabismus is often responsible for the development of amblyopia (2.3.3) [Wri06].

### 2.3.2 Refraction Error and Anisometropia

As already described in chapter 2.1, the curvature of the cornea and the lens are largely responsible for ensuring that images of the surroundings are sharply focused on the retina. This condition, also known as emmetropia, is illustrated in Figure 2.4(a). It is only possible when all refractive elements of the eye are healthy and match with each other [Atc00].

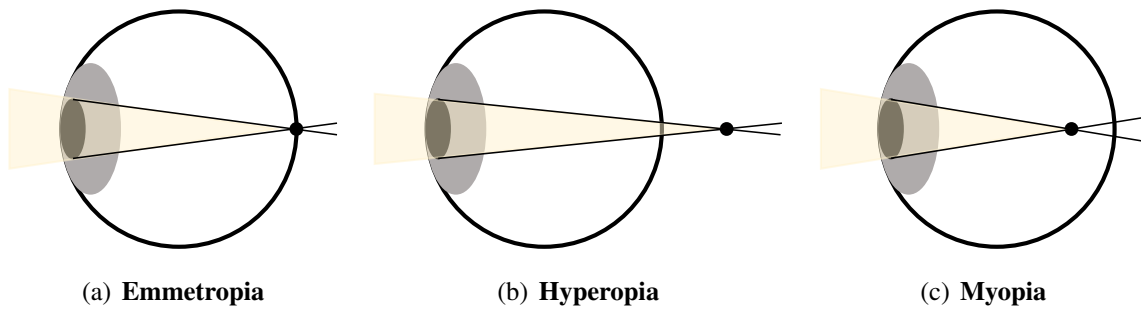


Figure 2.4: (a) represents the state of a healthy eye in which the light is focused on the retina. In (b) and (c), however, the light is focused behind and before the retina, because of refraction errors, based on [Har19].

If an eye is no longer able to focus on the retina, the object is outside the range of accommodation. This means that the lens cannot be deformed strongly enough to adapt to the needs of the eye. As soon as this accommodation area is no longer within the normal range of a healthy eye, the eye has a refraction error. This kind of error is generally understood as an imbalance between the refractive power and the axial length of the eye [Har19]. Depending on the type of refraction error, there are many different factors responsible for these errors. The two best-known refraction errors are myopia and hyperopia, also known as nearsightedness and farsightedness [Ver15].

An eye with hyperopia, also known as farsightedness, is no longer capable of sharply imaging near objects on the retina. The point of focus is behind the retina because the axial length of the eye is too short compared to its optical power [Atc00]. This relation is illustrated in Figure 2.4(b). The reason for this can be either a too short axial length of the eye or errors of the refractive elements. These include a cornea that is too flat or an insufficient lens strength [Har19]. In contrast, in eyes suffering from myopia, distant objects are imaged before the retina, represented in Figure 2.4(c). This is therefore nearsightedness, and the axial length of the eye is too long in contrast to its optical performance. In most cases myopia is a product of dysregulated eye growth [Har19].

Since the eyes are not able to focus the images directly on the retina in both refractive errors, blurred images are produced. However, in both cases, the eyes are to a certain extent able to compensate for the false refraction through stronger accommodation of the lens. But over time, this leads to side effects such as headaches and eye fatigue. Therefore, refraction errors are usually corrected at their origin by using glasses that can compensate the lack of refraction [Atc00].

A special characteristic of refraction errors is called anisometropia. Patients who suffer from anisometropia have a different refractive error in each eye. The difference can be just a different degree of refractive power in each eye, or both eyes have a different type of refractive error. This



means that one eye suffers from myopia while the other eye suffers from hyperopia. Since both eyes perceive two very different images due to anisometropia, subconscious suppression of one of the two eyes often occurs. For this reason, anisometropia often leads to amblyopia as well [Atc00].

### 2.3.3 Amblyopia

Amblyopia is a disease of the visual system, which affects about 1.3 % to 3.6 % of children and is the most frequent reason for monocular vision loss in adults [Bir13, Lev06]. Caused by a developmental disorder of the visual system in early childhood, amblyopia leads to lifelong visual deficits if not treated early enough [Bir13].

Amblyopia itself is not a disease that develops on its own, but always occurs in the presence of amblyogenic factors [Bir13]. The most common amblyogenic factors are strabismus (2.3.1) and anisometropia (2.3.2). These visual malfunctions obstruct the development of the visual system by degrading the retinal images [Hol06]. The two main reasons for the deteriorated images are blurred vision, due to anisometropia, or faulty binocular interaction caused by strabismus [Hol06]. For both factors, the degradation of the image refers mainly to the amblyopic eye, which subsequently gets suppressed, as mentioned in chapter 2.3.1 and 2.3.2. Due to the worse or even complete absence of visual information in the amblyopic eye, caused by suppression, binocular vision deteriorates drastically and so does stereopsis [Haa03, Bir13].

Since amblyopia is not the cause of low vision, more than just the presence of poor visual acuity together with amblyogenic factors must be considered for diagnosis. In order to make a solid diagnosis of amblyopia, visual acuity must be tested after all visual dysfunctions caused by amblyogenic factors have been corrected. Such corrections include, for example, the wearing of glasses. If the visual acuity is still not within normal range and there are no other visual system dysfunctions that could reduce the visual acuity, it is considered to be amblyopia. Since the sensitive development phase of the visual system is in the first seven years of life, an early diagnosis is particularly important to enable targeted therapies [Hol06].

### 2.3.4 Treatment of Amblyopia

In addition to an early diagnosis of amblyopia, rapid therapy is urgently needed. Without appropriate therapy, irreversible loss of vision can occur. In addition to the resulting general limitation in everyday life, unilateral vision increases the probability that the only healthy eye left

will become diseased or even completely blind [Bir13, Haa03].

It is not possible to determine the ideal period of time for therapy in a generalized way, as each individual responds differently to therapy. But clinical trials have shown that on average, children aged 3 to less than 7 years achieved greater improvement in visual acuity after therapy than children aged 7 to less than 13 years. It is also thought that with severe amblyopia, the positive response to therapy decreases more steeply with increasing age [Hol11].

Before starting the actual therapy for amblyopia, all amblyogenic factors must be eliminated as far as possible. In many amblyopic patients, the use of glasses alone leads to an improvement in visual acuity. If there are no other anatomical deficits that can be compensated, the actual therapy of amblyopia begins. Since the main problem with amblyopia is the suppression of the amblyopic eye, the therapies aim to degrade or completely remove the visual input of the healthy eye. As a result, the amblyopic eye is no longer suppressed and by using it, there is the possibility to train its visual acuity [Hol06].

The existing treatments can be divided into monocular and binocular therapy. In monocular therapy, only the amblyopic eye is used. The best known and most widespread form of this therapy is patching. It has been used for several centuries and has been proven to enhance the visual acuity of the amblyopic eye. The principle of the treatment is to completely cover the healthy eye with a patch. This forces the patient to use the amblyopic eye to perceive and interact with the environment. To achieve success with patching, regularity and frequency of use is crucial. However, the length of time the patch is worn as prescribed by the doctor can vary from half an hour to several hours per day [Hol06]. Even if patching leads to a positive visual acuity result in the majority of children, it remains a monocular therapy that focuses solely on improving visual acuity. Thus, during the period of patch application, cooperation between the two eyes is still not supported. Consequently, improvements in binocular vision and stereopsis are largely absent. Therefore, binocular therapy focuses primarily on improving binocular vision and stereopsis. By improving them, visual acuity should improve on its own as a secondary consequence [Hes15]. The basis of this type of treatment is based on more recent studies about the disease, which suggests that the main problem of amblyopia is not the weakness of vision, but the lack of binocular interaction.

This also seems to be the reason why amblyopia is often not completely cured, although success has been achieved in the visual acuity [Bir13]. For this reason, binocular therapy does not aim to shut down the healthy eye completely but to deteriorate its vision only to the extent that the suppression of the amblyopic eye is eliminated. The patient is then given special tasks that can

only be solved if both eyes work together, whereby binocular vision takes place. The aim of the therapy is to reverse the deterioration of the healthy eye subsequently until it can be completely removed without suppression taking place [Bir13, Hes15].



# Chapter 3

## Related Work

As already mentioned in chapter 2.3.4, there are many different approaches and procedures for the treatment of amblyopia, divided into monocular and binocular therapy. In the following, some of these treatments are briefly presented.

### 3.1 Monocular Treatment

There are a variety of monocular therapy approaches, all of which aim to restore the monocular function of the amblyopic eye. The basis of these therapies is to prevent the healthy eye from seeing in order to reverse the suppression of the amblyopic eye [Hes15].

As mentioned above in chapter 2.3.4, patching is probably the longest known treatment for amblyopia and is still the most widely used today. In addition to patching, there are also atropine drops used, which achieve similar results as patching and are mostly used as a replacement when the patches cannot be worn due to skin irritations. They have a paralyzing effect and when they are applied to the healthy eye, it is no longer able to adjust the refractive power of the lens to enable the eye to fixate on a certain object. As a result, the healthy eye perceives almost as little as if it is covered with a patch. For this reason, all therapies that use patching or atropine are entirely monocular therapies, as they create purely monocular conditions [Hol06].

Due to very poor compliance with long-term patching, there are numerous therapies that reduce the daily periods of patching by actively using the eye during this time. In order to increase tolerance and cooperation of the patient, a therapy was published in 1978, which is limited to a short-term occlusion of 20 minutes per day. To further increase the success, visual stimuli, in form of rotating grids, were used to activate all visual neurons, thus providing maximum training for

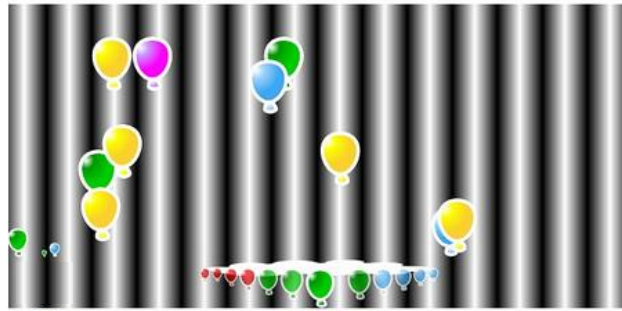


Figure 3.1: The screenshot shows the structure of a game from Caterna. The black and white grid pattern in the background represents the stimulus, while the colored balloons in the foreground are used to perform certain tasks, based on Caterna Vision GmbH<sup>1</sup>.

the amblyopic eye. To ensure that the patient looks at the stimulus for as long as possible during the 20 minute therapy, the stimulus is generated behind a transparent cover on which the patients can play drawing games meanwhile [Cam78].

A more recent and patented amblyopia therapy based on the principle of short-term occlusion published in [Cam78] is offered by Caterna [A.1]. In the so-called vision school, a patch must be worn on the non-amblyopic eye during therapy as well. The big difference to the therapy of 1978, is the digitalization of the application. The attention of the patients is directed to the screen of a monitor, on which they can play various games. Stimuli are again displayed in the background of the games as illustrated in Figure 3.1. Which stimuli and in which frequency they should occur is individually adjusted to each patient and can also be changed in the course of the therapy. The recommended period of use is between 30 and 45 minutes per day [A.1].

The short-term occlusion has increased patient acceptance and success in the visual acuity of the amblyopic eye. Nevertheless, there are still negative experiences and results of these therapies. Even though acceptance has increased due to short-term occlusion, it is difficult for children to understand why the healthy eye is covered and they have to work with the worse eye [Sea00]. Besides the negative psychological influences on the therapies, there are also considerations from a medical point of view. While the visual acuity of the diseased eye improves with the help of therapy, the visual acuity of the healthy eye is reduced because the eye remains inactive and without learning opportunities during the period of non-use. In addition, stereopsis does not lead to any success, since at no time, neither during the patch phase nor during the phases when the patch is removed, can both eyes see and work together at the same time [Hol06]. For this reason there are now more and more therapeutic approaches that try to make binocular vision possible.

---

<sup>1</sup><https://caterna.de/>

## 3.2 Binocular Treatment

The binocular treatment is mainly aimed at eliminating the suppression of the amblyopic eye in order to train binocular vision. By removing the suppression, both eyes can work together and learn to fuse and process all information correctly. There are different methods to enable both eyes to work together. Most are connected with recent, digital technology. Some of these are presented below, all of which are based on the principle of providing different inputs to each eye.

VR technologies contain an important component for the implementation of binocular therapy. It has the advantage that each eye looks at its own screen, which allows two different images to be displayed to the patient. Already in 2006 this technological achievement was used for the binocular treatment of amblyopia.

The structure of such a computer system and how it can contribute to the therapy of amblyopia is described in the paper by Eastgate et al. [Eas06]. The basis of this binocular therapy approach, using the VR technology, is the possibility to show both eyes two different images, which are individually modified. The therapy itself is designed as a video game. During the game, the same background is displayed on both screens. However, some important elements of the game process are only displayed on the screen, which is viewed exclusively by the amblyopic eye. Furthermore, it is possible to adjust the squint angle individually for each patient. This makes it possible to compensate existing strabismus of the amblyopic eye by shifting the displayed image by the squint angle so that both eyes receive similar retinal images. One of the games modified for this purpose is Pac-Man. The moving components of the game, the Pac-man and the ghosts are only displayed to the amblyopic eye, whereas the walls of the labyrinth are mainly displayed to the dominant eye. To allow a fusion of both images parts of the labyrinth are added in the amblyopic eye as well. To complete the game successfully it is necessary that both eyes work together. It is almost impossible to complete this task while one of the eyes is suppressed. This Interactive Binocular Treatment (I-BiT) system was tested in a study on amblyopic patients, in which significant improvements in visual acuity were achieved throughout the study [Her16]. However, the entire structure of the system described by Eastgate et al. is designed for a physician to make individual settings for the patient on a second screen while the patient is undergoing therapy. Because of this, the system in this form is not suitable for daily use at home.

A current patented application based on the just mentioned method, of showing both eyes different images, is offered by Vivid Vision[A.2]. This therapy is also an interactive video game that can be played on VR headmounted displays (HMD). In order to offer a certain amount of variety, and thus prevent a lack of interest, there is a wide range of possible games. All are based

on the principle that the background is the same for both eyes, but important elements are only visible to one eye. It is also capable of compensating for strabismus and reducing the image quality of the healthy eye in order to adjust both eyes to each other. The system has the advantage that it is suitable for use at home and the results can be viewed online by the doctor. A study also showed a significant increase in visual acuity when the Vivid Vision system was used by adults [Žia17].

A binocular therapy patented by Amblyotech Inc also works with the principle that both eyes receive different images and can only win the game if both eyes work together [A.3]. However, this game is designed for mobile devices such as iPads and smartphones. As these devices have only one screen, all the elements necessary for the game must be displayed together on one screen. In order to ensure that each eye can only partially perceive elements of the game, they are displayed in the complementary colors red and blue. With the help of anaglyphic glasses, the eyes are only able to see the colors that do not correspond to their lenses. In addition, the system is also able to equalize the image qualities of both eyes, by displaying the color assigned to the healthy eye with different intensities. A study by Kelly et al. compared the iPad game with pure patching. In the study, one group used the iPad game independently at home at regular intervals over two weeks for a total of 10 hours. The subjects in the other group had to wear patches for 2 hours every day during the two weeks. Although the patches were used more often than the iPad game, the iPad group achieved greater improvements in visual acuity [Kel16]. Despite the positive results as a home therapy for strabismus patients, additional prisms are needed to be attached to the glasses to compensate for the squint angle. But the compensation of the squint angle cannot be adjusted to the achieved improvements of the therapy in every application, since an additional squint angle measurement is necessary to select the appropriate prism and not everyone has the possibility to measure this at home.

Both Amblyotech Inc and Vivid Vision offer successful binocular therapies to use at home. While the Amblyotech Inc method provides an inexpensive and simple application, the Vivid Vision therapy offers next to the actual therapy the possibility to regularly recalculate the squint angle and the degree of suppression on one single device. In addition to these two methods, other binocular therapies are mentioned in the literature, which work similarly and are based on presenting different images to both eyes. What is missing, however, is a system that can be used at home, in which both eyes receive the same images and are trained by playing purely stereoscopic tasks to improve stereoscopic vision and visual acuity. Accordingly, this thesis



presents a binocular VR-Amblyopia Trainer, which shows exactly the same scene to both eyes and trains them with a purely stereoscopic task. The only differences in the images refer to the adjustment of the squint angle and the image quality. Accordingly, the system also has the ability to calculate the squint angle and the degree of suppression on the same device.



# Chapter 4

## Methods

This chapter is divided into three parts. First, the used VR HMDs are presented, highlighting their commonalities and differences. Secondly, the used VR-Amblyopia Trainer is described in detail, followed by the modifications that have been applied to make it work on the standalone device. Subsequently, the study design is outlined, in which the two devices were compared concerning the VR-Amblyopia Trainer. And finally, it is mentioned how the raw data obtained in the study were further processed.

### 4.1 HTC Vive Pro and HTC Vive Focus Plus

The original version of the VR-Amblyopia Trainer, described in 4.2, works on the VR HMD HTC Vive Pro<sup>1</sup>. However, the setup of the Vive Pro is very extensive and complex due to additional hardware components, namely the high-performance computer and external tracking stations. To make the application more flexible and easier to use, it was adapted to a standalone device, the VR HMD HTC Vive Focus Plus<sup>2</sup> in the course of this thesis. In the following, the two devices are compared with each other in order to list both similarities and differences.

The two main components of both systems to interact with the virtual environment are the HMDs and the controllers. The characteristics of the HMDs are mostly identical for both devices. Both headsets have a Dual AMOLED 3.5" display with 1.440 x 1.600 pixels per eye and a field of view of 110°. Differences in the displays relate to the refresh rate and the pupil distance. While the refresh rate of the Vive Pro is 90 Hz, the Vive Focus Plus has 75 Hz. Furthermore, a desired

---

<sup>1</sup><https://enterprise.vive.com/de/product/vive-pro/>

<sup>2</sup><https://enterprise.vive.com/de/product/focus-plus/>

interpupillary distance can be set on the Vive Pro with an accuracy of 0.1 mm between 61.2 mm and 73.0 mm. On the other hand, only five distances between 60.5 mm and 74 mm can be selected for the Vive Focus Plus. The individual values are roughly 60.5 mm, 63.9 mm, 67.3 mm, 69.2 mm and 74 mm.

To ensure that the system is always able to locate the headset and the controllers in the room, the Vive Pro uses Lighthouse as a tracking system. This requires at least one additional base station, which must be recalibrated each time its position is changed. The base station sends out laser beams and synchronous pulses, which enables the tracking system to determine the positions of the sensors with sub-millimeter accuracy through triangulation. With the help of a high-speed inertial measuring unit, it is also able to determine speeds and orientation with a sampling frequency of up to 1000 Hz. In contrast, the Vive Focus Plus requires no additional tracking stations in the room. The position of the controllers in relation to the headset is determined by ultrasonic pulses generated within the HMD and sent to the controllers. The resulting data can be used to determine the 3D position information with sub-millimeter precision as well.

The Vive Focus Plus is a standalone device and requires no hardware other than the HMD and controllers, as the HMD has a Qualcomm Snapdragon 835 processor that runs all processes on the device. The Vive Pro, on the other hand, is permanently connected to a powerful computer that performs all calculations for the headset. As the computer must meet special prerequisites, a computer with an AMD Ryzen Threadripper 1950X 16-Core Processor and NVIDIA GeForce RTX 2080 Ti was used in this study.

The Vive Focus Plus has special advantages due to the greatly reduced hardware components. With no additional tracking systems that need to be recalibrated in each room and no high performance computer, the device is reduced in costs and easier to use.

## 4.2 VR-Amblyopia Trainer

The following chapter is about the VR-Amblyopia Trainer, in which VR technologies are used to realize a binocular therapy for amblyopia. In contrast to the binocular therapies described in 3.2, the VR-Amblyopia Trainer focuses on presenting both eyes the same scene without showing individual elements only to one eye. The only difference between the two images is the adjusted image quality and a possible displacement due to a squint angle. To ensure that the patient still works continuously with both eyes, the training situation is about recognizing depth relationships. Since stereoscopic vision is only possible, as described in chapter 2.2, if the retinal images of both



Figure 4.1: **Main menu.** The different levels are represented with pictures on the wall. Below left the strabismus level, below right the suppression level and above the stereopsis level in three different environments. Each level can be selected by pointing the controller at the corresponding image and pressing a button.

eyes are compared, the game can only be successfully completed by using both eyes.

The VR-Amblyopia Trainer is structured like a game and divided into three levels. The strabismus level measures the patient's squint angle and the suppression level calculates the contrast by which the image quality of the healthy eye has to be reduced in order to avoid suppression. The therapy should always start with the strabismus level or suppression level. Whether the squint angle or the necessary contrast is calculated first depends on the patient's individual clinical history. The actual therapy takes place at the stereopsis level. To ensure binocular vision at this level, the system automatically adjusts the images of the amblyopic and healthy eye, based on the previously calculated squint angle and image quality, to avoid suppression and allow fusion of the retinal images.

After starting the application, the user is initially located in the main menu, shown in Figure 4.1. From the main menu, all levels can be entered in any order and after completing a level, the user always returns to the main menu and can enter the next level. The entire game can be operated completely independently by using the controllers. With the Vive Focus Plus, only the user is able to operate the game by using the controllers. With the Vive Pro, on the other hand, there is the additional option of using the computer keyboard to make the same entries as with the controllers.

The entire game process and the environment is implemented in the game engine Unreal Engine 4<sup>3</sup>. General settings regarding the measurement conditions and the game procedure can be

<sup>3</sup><https://www.unrealengine.com/en-US/>

set in an external Ini file. This allows various settings to be changed quickly and easily, which makes the program more user-friendly for people who are not familiar with the system. The following chapters specify which settings are available in the Ini file individually for each level.

### 4.2.1 Strabismus Measurement

The strabismus level is capable of measuring a squint angle by using two identical looking stimuli. The stimuli consist of one cross and four basketballs, one placed on the right, one on the left, one above, and one below the cross, as shown in Figure 4.2(a). The first of the two stimuli is projected in one of the nine directions of gaze, also called azimuth and illustrated in Figure 4.2(c). This stimulus cannot be moved and is only visible to the eye whose squint angle is not to be measured. The other stimulus is displayed offset either to the right, left, above, or below the azimuth in which the first stimulus is located. The offset displayed stimulus can be moved in the four main directions up, down, right and left and is only visible to the eye whose squint angle is to be measured. Figure 4.2(b), represents the two offset stimuli. In the actual game, both stimuli look the same. The green items have only been colored to illustrate, which objects can be perceived by the same eye. Furthermore, both stimuli are projected at a distance of 112 cm to the viewing position and additionally, they are displayed in such a way, that they do not change their position relative to the eyes when the HMD is moved by turning the head. Especially users without strabismus are not able to fuse the images of both retinas under these initial conditions. This is due to the fact that the stimuli are initially located at two different positions, and thus

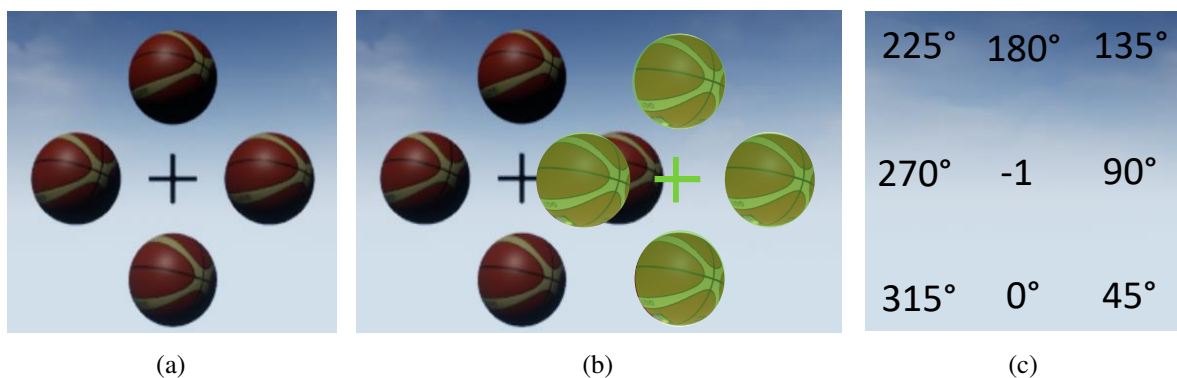


Figure 4.2: **Strabismus stimulus.** (a) The stimulus consists of 4 identical balls arranged evenly around one cross. (b) Each stimulus is only visible in one eye. The green colored stimulus is displayed offset to the other, causing double images to be perceived. This stimulus can be moved in the four main directions. In the correct application, both stimuli have the same colors. (c) represents the designations for the nine different azimuths, in which the stimuli are displayed.

are imaged at non-corresponding retinal points. As explained in chapter 2.2, this leads to the perception of double images.

The task of the user consists of shifting the movable stimulus in the direction of the stationary one until both retinal images fuse and thus only one stimulus can be seen. The stimulus has to be shifted by using the trackpad on the controllers. The trackpad can be pressed in one of the four main directions to move the stimulus in the corresponding direction. If it is pressed only once briefly, the stimulus moves one step. If, on the other hand, it is pressed longer, the stimulus moves continuously in the corresponding direction until the button is no longer pressed. After the retinal images fused, this must be confirmed by pressing another button on the controllers.

In order to additionally determine whether strabismus only occurs in certain directions of gaze or permanently, the squint angle is measured in the nine different azimuths, illustrated in Figure 4.2(c). However, due to the panum's fusional area, described in chapter 2.2, the retinal images already fuse even if the two stimuli are not yet projected to corresponding retinal points. Therefore, no reliable squint angle can be calculated from a single measurement. In order to measure the actual squint angle as far as possible without the influence of the panum's fusional area, the movable stimulus must be shifted from different directions towards the stationary stimulus. At azimuths  $-1^\circ$ ,  $45^\circ$ ,  $135^\circ$ ,  $225^\circ$  and  $315^\circ$  the movable stimulus has to be shifted once from above,

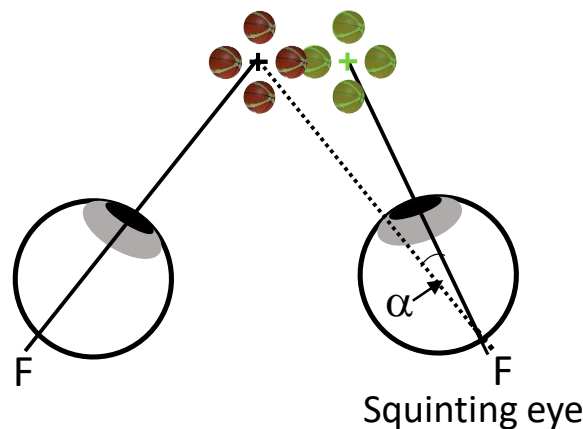


Figure 4.3: **Perception of stimuli with strabismus.** The stimulus not colored green corresponds to the stationary one and is only visible to the left eye. The left eye is aligned in a way that the stimulus is imaged on the fovea. The broken line going from the stationary stimulus through the fovea of the squinting eye is meant to represent how a healthy eye would be aligned. The green colored stimulus is the movable stimulus and can only be perceived by the right eye, the squinting eye. Although the stimulus is not in the same position as the other one, it is still imaged on the fovea due to the eye position. The angle  $\alpha$  between the broken and solid line corresponds to the squint angle of the eye.

from below, from the right and from the left. Since the remaining azimuths are located on the horizontal or vertical viewing directions of the eyes, the stimulus is shifted there only from two directions. At azimuths  $0^\circ$  and  $180^\circ$  it has to be shifted from below as well as from above and at azimuths  $90^\circ$  and  $270^\circ$  it has to be shifted from right and from left towards the stationary stimulus. This means that in each of the measured directions the confirmed position is affected by the panum's fusional area. Based on the measured positions, the corresponding squint angle can be calculated by determining the mean value, which ideally is not influenced by the panum's fusional area anymore.

To calculate a squint angle from this procedure, the horizontal and vertical distances between the cross of the stationary stimulus and the cross of the movable stimulus are always measured after the position has been confirmed with the controller. The fixed stimulus is the target position and thus the reference position for the calculation. The vertical and horizontal difference between the two image positions is then used to calculate the squint angle. If the stimuli are placed in the same position, there is no distance between them. Thus exists a squint angle of  $0^\circ$ . However, if a user has a squinting eye, it is impossible to superimpose the two images correctly. This is because, due to the different orientations of both eyes, the stimuli are mapped on corresponding retinal points when the stimuli are at offset positions. This offset position corresponds to the squint angle of the eye and is illustrated in Figure 4.3. The methodology of strabismus level is also published by Mehringer et al. [Meh20].

**Setting options in the Ini file:** The Ini file offers the possibility to determine whether only the amblyopic eye or both eyes should be checked for a squint angle. If both eyes are to be checked, twice as many measurements are taken. Furthermore, it can be defined which directions of gaze are to be checked. To improve the significance of the results, it can be set how often the average squint angle should be calculated per direction of gaze. In other words, how often the stimulus should be moved from the different directions in one azimuth. Finally, it can also be specified whether the calculated squint angle is only applied in the stereopsis level in order to shift the projected image accordingly, or also in the suppression level.

## 4.2.2 Suppression Measurement

The suppression level is used to determine a certain contrast, which reduces the image quality of the healthy eye to such an extent that the suppression of the amblyopic eye can be eliminated. In this case, the image quality is reduced by using different contrasts, which are implemented in the form of a transparent grey veil.



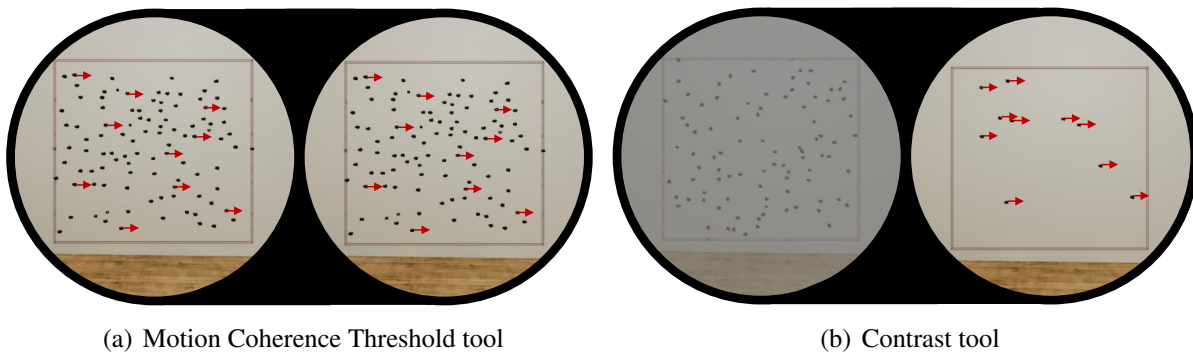


Figure 4.4: **Suppression Stimulus.** It is illustrated what both eyes are shown during which tool. In (a), both eyes receive the same animation. In this example, there are one hundred points, 10 % of which (represented by red arrows) move to the right. In (b), a Motion Coherence Threshold of 10 is displayed to the right eye, which moves to the right. The left eye only receives the remaining points, randomly moving. Additionally, a contrast is added to the left eye.

The measurement is divided into two parts. In the first part, both eyes receive exactly the same images. A fixed number of points appear on the screen, all moving in the same direction. The possible directions of movement are up, down, right and left. The direction of movement of the points should then be indicated with the trackpad on the controller. If the answer is correct, only a certain percentage of points move in one direction, and the remaining points move scattered in all directions. The number of points moving in one direction is reduced after each correct answer and increased after each incorrect answer. The aim is always to identify the direction in which most are moving. In addition, the program stores for each answer the percentage of points moving in one direction. Figure 4.4(a) illustrates the images received from both eyes. For a better understanding, the red arrows have been added to the image to indicate which points are moving in the same direction. The measurement is automatically terminated when there is a change between the correct and incorrect inputs for the sixth time. Subsequently, the mean value is calculated from all stored percentages that occurred after the first wrong input. This value is called Motion Coherence Threshold (MCT), which is also the name of this measurement tool. The methodology to measure the motion coherence threshold has already been described by Wattam-Bell [Wat94].

The second measurement, called contrast tool, determines the degree of suppression. Accordingly, it calculates the necessary contrast so that the amblyopic eye can detect the direction of motion if the number of points in one direction corresponds to the previously calculated MCT. This time, both eyes receive different images. The amblyopic eye sees the percentage (MCT) of points moving in the same direction. At the same time, the healthy eye only receives the remaining points that are moving in random directions. Additionally, a contrast is superimposed on the

image of the healthy eye. The images received by each eye are illustrated in Figure 4.4(b). At the beginning of the measurement, the contrast is set to 0 %, which means that the healthy eye only sees a grey veil, since the contrast difference is maximum. If the answers are correct, the contrast is increased in small steps. Once a certain contrast is reached, especially amblyopic patients are no longer able to determine the direction of movement. This is based on the fact that the image quality of the healthy eye is again good enough to suppress the amblyopic eye. Accordingly, the contrast is reduced again in the case of incorrect answers. This measurement is also terminated after the sixth change between incorrect and correct entries. As in the MCT, the mean value is calculated from all the contrasts tested after the first false input. This mean contrast is saved and applied to the healthy eye in the other levels. The contrast tool can also be calculated the other way round. This means that the grey veil is still on the healthy eye, but the healthy eye now receives only the points moving in one direction, and the amblyopic eye sees all the remaining points.

**Setting options in the Ini file:** It is possible to specify whether the calculated contrast should only be applied in the stereopsis level or also in the strabismus level. The settings that apply to both, the Motion Coherence Threshold tool and the Contrast tool are as follows: It can be defined how many points should appear in total. This number usually corresponds to 100. The level of difficulty can be varied by setting whether the points are only visible for a limited time, at what speed the points should move and in which radius around a point no other may appear. In addition, it can be specified after how many switches between correct and incorrect inputs the measurement should be terminated and how often each measurement should be performed. If the tools are executed more than once, the average of the results is used for further progress. For the motion coherence threshold tool, it can be defined how many correct answers are needed to increase the difficulty level. For the contrast tool, it can be defined as well how many correct answers are needed to increase the contrast. Additionally, it can be determined whether both eyes should be tested for contrast or only the amblyopic eye.

### 4.2.3 Stereopsis Level

When entering the stereopsis level, the program automatically sets the required contrast and the compensation of the squint angle, which were measured in the two previous levels. This should enable amblyopia patients to merge the retinal images of both eyes and thus gain binocular vision. At the stereopsis level, the user is placed in the middle of a room with a table in front of him, as shown in Figure 4.5. Additionally, one of the controllers no longer has its own appearance in the HMD but looks like a table tennis racket.



Figure 4.5: **Stereopsis level.** The user is placed in front of a table. From the opposite side of the table, two balls fly towards the user at the same time.

A run begins with one ball dropping vertically down onto the end of the table, about 214 cm from the user away. When touching the table, the ball splits into two balls that bounce off the table and fly towards the user. The balls are not at the same distance from the user, but one is a little further in front than the other. The distance between the two balls is called disparity, which allows stereoscopic vision as described in chapter 2.2. The task of the user is to touch or hit away the ball closest to the user with the table tennis racket. The reaction time can vary since the user is able to lean forward or backward and thus touch the ball sooner or later. However, the decision time is limited, since the balls can fly past the user and can then no longer be touched. If a ball has been touched or the balls have flown past the user, they disappear again. This is the end of one run. The next run starts randomly after one or two seconds when a ball appears on the opposite side of the table and falls back down.

The setup of the environment prevents that the recognition of the correct solution is facilitated by monocular indications of depth information. To achieve this, it is ensured that the two balls do not overlap and do not cast shadows, thus the task can only be solved binocularly. Additionally, the positions of the balls in the x, y and z directions are adjusted so that the viewing angles on the two balls are the same. In this way, no conclusions can be drawn about the depth position of the balls based on the trajectory.

Due to smaller disparities and greater speed, the difficulty can be varied. Besides, the contrast can be varied during the game, which can change the level of difficulty as well. In amblyopic patients, however, it must be taken into account that the adjusted contrast is usually already the upper limit, and a further increase of contrast may prevent binocular vision again. If the

VR-Amblyopia Trainer is used successfully, the required contrast should increase with each measurement until finally a contrast of 100 % is reached and the amblyopic eye is still not suppressed.

**Setting options in the Ini file:** For the stereopsis level, a total of three settings can be defined via the Ini file. Several disparities can be determined, which are used in random order during the game. It can be defined how often each of the defined disparities should occur, and to change the difficulty level, the playing speed can be adjusted as well.

### 4.3 Modification for the Standalone Device

For the VR-Amblyopia Trainer to achieve success in therapy, it is important to be used regularly. However, as mentioned in chapter 4.1, the Vive Pro requires a lot of additional equipment and starting the game is complicated for inexperienced users. To overcome these issues, the aim of this thesis was to modify and adapt the VR-Amblyopia Trainer to run on a standalone device, the Vive Focus Plus. This chapter describes the modifications made for this purpose.

Unlike the Vive Pro, the Vive Focus Plus is an Android based device. For this reason, the SteamVR<sup>4</sup> plugin had to be switched to the WaveVR<sup>5</sup> plugin, as Vive Wave is specifically designed to develop for Android and mobile VR. Together with the Wave SDK, the plugin offers different VR headsets the possibility to easily access the created content. But since the Wave Unreal SDK is not automatically included in Unreal Engine, it had to be integrated manually. In order to interact with the controllers during the game, a blueprint provided by the SDK had to be inserted into each level. This blueprint is able to identify the connected controller model and display the corresponding design in the headset. Therefore it is possible to use the application with different controller models without having to change the design for each model inside of Unreal Engine.

Since the computing power of the Vive Focus Plus is lower, settings regarding the high rendering requirements had to be changed to enable a smooth and realistic run through good rendering performance. To meet these prerequisites, firstly the VR Multiview feature was enabled, which is a VR-specific rendering mode provided by Unreal Engine that supplies the mobile device an optimized path for stereo rendering. In addition to the VR Multiview, OpenGL ES 3.1 was used as the standard software interface for graphics processing hardware.

---

<sup>4</sup><https://www.steamvr.com>

<sup>5</sup><https://developer.vive.com/us/wave/>

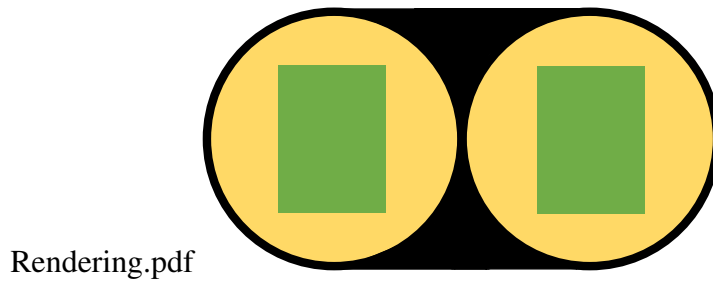


Figure 4.6: **Foveated rendering.** The green rectangle represents the foveated region, where everything is shown very sharp and the size of the rectangle can be varied. The yellow area represents the peripheral region, whose resolution is lower and can be set to low, medium or high. Based on VIVE Wave<sup>6</sup>.

In order to save additional computing power, computationally intensive materials were replaced or completely removed. Furthermore, the Foveated Rendering function was applied to save power and improve rendering performance as well. Foveated Rendering, illustrated in Figure 4.6, offers the possibility to define an area around the center of view, in which a high resolution is maintained. On the contrary, the resolution and thus the quality of the peripheral region is reduced and can be set between low, medium or high. This means that the entire room does not have to be displayed in sharpness, but only the region in the room that is actually being viewed.

Independently of the rendering performance, the application was supplemented by the following settings to simplify usability. The original version offers the possibility to cancel any level

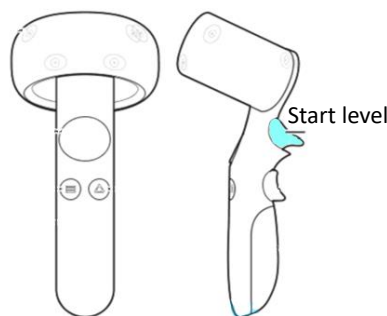


Figure 4.7: **Controller instruction.** The image for the stereopsis level is shown as an example for the instructions. The blue button must be pressed in the level to start the task. Based on Vive Wave<sup>7</sup>.

<sup>6</sup>[https://hub.vive.com/storage/docs/en-us/UnrealPlugin/Unreal\\_FoveatedRendering.html](https://hub.vive.com/storage/docs/en-us/UnrealPlugin/Unreal_FoveatedRendering.html)

<sup>7</sup><https://www.vive.com>

early, by pressing Esc on the computer keyboard. Since there is no additional keyboard on the Vive Focus Plus, a key combination of the controller inputs was added, by which each level can be canceled prematurely as well. In addition, a picture of the controllers was inserted at the beginning of each level. On the picture, for each level individually the controller buttons are color-coded, which have to be pressed for each action in the current level. Figure 4.7 shows an example of the stereopsis level. The goal of this integrated guide is that the VR-Amblyopia Trainer can be used completely independently.

After the program was ready customized, it was packaged to create one single package of all necessary files, that can be installed on the headset without further effort. After successful installation, the VR-Amblyopia Trainer can be opened normally like an app from the headset's start menu. In order to access the settings in the Ini file and the saved results, the headset must be connected to a computer, which does not need any special features. After connection, the required files can be accessed on the computer via predefined file paths.

## 4.4 User Study

To compare the functionality of the modified VR-Amblyopia Trainer with the original version, a repeated measure study was conducted. This specifically involved the comparison of the results obtained during the game, as well as the questionnaires filled in afterward. The following chapter presents the details of the study, divided into an overview of the participants and into the course of the study.

### 4.4.1 Participants

A total of 20 subjects (ten male, ten female) with an average age of  $22.65 \pm 1.88$  years participated in the study. Exclusion criteria for participation were the two diseases manifest strabismus and amblyopia, as well as a visual acuity of less than 0.5 VAdc. 14 subjects had a dominant left eye, and the remaining six had a dominant right eye. The dominant eye was determined during the study, and the process is described in 4.4.2. In addition, eight of the 20 subjects claimed to be myopic. These wore their own doctor-prescribed glasses or contact lenses during the study, which compensated for the refractive errors. Only three of the subjects had major experience with VR.

### 4.4.2 Procedure

The study design, illustrated in Figure 4.8, corresponds to a repeated measure design with a time gap of one week between the two runs. Each group consisted of five female and five male subjects. The difference between the two groups was the order in which the devices were tested. While group 1 used the Vive Pro in the first run, group 2 started with the Vive Focus Plus. At the beginning, all participants regardless of which group were given a short introduction about the course of the study, they had to sign a consent form and fill out a questionnaire regarding their demographic data.

Before the actual measurements and data acquisition could begin, the dominant eye had to be determined. The subjects were asked to form a circle with thumb and index finger and to look through the circle with both eyes. They had to align the circle in a way that a red X on the wall could be seen through the circle. Under these initial conditions, they had to close the right eye and the left eye one after the other. While one of the eyes was closed, they were asked whether

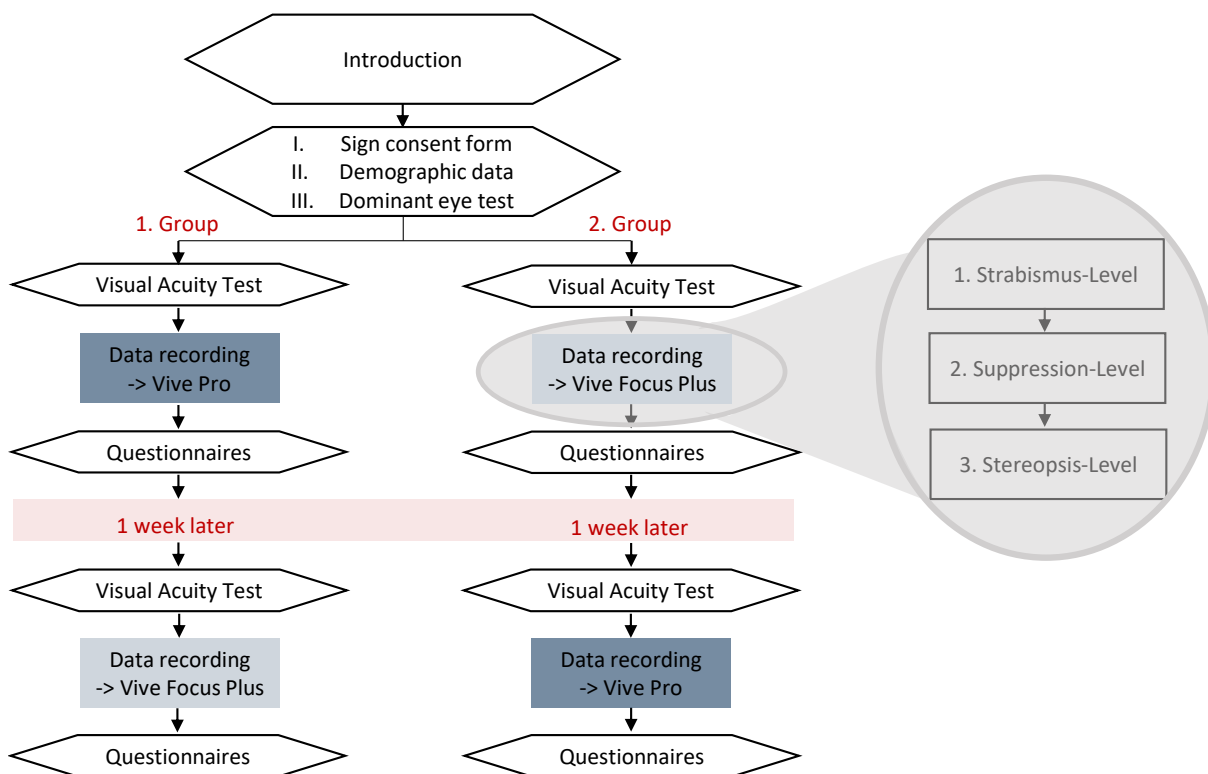


Figure 4.8: **Study design.** The study design for both groups is shown in the flow chart. Each group consisted of five female and five male subjects. The data recording procedure was the same for both devices and as questionnaires were filled out the SuS and the IPQ.

the X is still in the circle. If the answer was yes while the left eye was closed, the right eye was the dominant eye. The dominant and therefore also non-dominant eye was determined since only subjects without amblyopia participated in the study. In the Ini file, however, it is necessary to specify which eye is the amblyopic eye, since the program adjusts all necessary settings to the right or left eye based on this information. For this reason, the non-dominant eye was entered individually for each subject as the amblyopic eye to create identical baseline conditions between the subjects.

In addition to the dominant eye, the visual acuity of both eyes was determined, using the Freiburg Vision Test by Michael Bach [Bac06], with a distance of four meters from the screen and a darkened room. The test was performed individually for each eye and each subject started with its dominant eye while the other one was closed. After a short break, the other eye was tested. This procedure was repeated three times to obtain a reliable average from the values.

Before the data recording of the VR HMDs began, all subjects received a briefing on the hardware of the controllers to ensure that all necessary buttons and their positions were known. Additionally, the interpupillary distance was adjusted to the subject's gender. It was not measured and set individually for each subject, as the Vive Focus Plus can only be set to five different distances. The average interpupillary distance of 60 mm was used as a guideline for women and 64 mm for men. Accordingly, the distance closest to the guide value was first selected for the Vive Focus Plus. For women, this corresponded to the smallest step of 60.5 mm and for men to the second step of about 63.9 mm. The Vive Pro was then set to these values to ensure comparability, even though the values of the Vive Pro could have been set more precisely. For men 63.9 mm could be set, for women only 61.3 mm, as this is the smallest possible adjustable interpupillary distance.

After the headset was put on, the subjects were located in the main menu. Everyone was given a familiarization period to get used to the virtual environment and the movement of the controllers. Subsequently, the subjects were instructed to sequentially enter the strabismus level, then the suppression level, and finally the stereopsis level using the controllers. At the beginning of each level, everyone got a briefing about the task. To obtain comparable results of the two devices, the settings in the Vive Focus Plus Ini file were the same as those on the Vive Pro. In the strabismus level, it was determined that a squint angle should be calculated for both eyes, whereby each of the nine directions of gaze were tested only once for each eye. In the suppression level, the MCT and contrast were each measured twice and the contrast in the contrast tool was only calculated on the healthy eye. At the stereopsis level, three disparities (275, 550, 825) were defined, each of which was tested 16 times. Accordingly, a total of 48 balls were played. However, at the beginning of



the stereopsis level, all subjects played ten runs to get a feeling for the interactive task. The results of these ten training runs were not saved and subsequently, the actual 48 runs began. After the last level was finished, two questionnaires the System Usability Scale (SuS) [Bro96] and the Igroup Presence Questionnaire (IPQ) [Sch03] had to be filled out digitally on the computer.

The second run with the other device was not carried out directly afterward, but exactly seven days later. The break was inserted so that any learning effects from the first run would have disappeared again and that thereby the starting conditions for both devices could be as equal as possible. The second run started with the visual acuity test on the same eye. The Vive Focus Plus was used by group 1 and the Vive Pro by group 2.

## 4.5 Data Processing

As described in 4.2, different measurements were taken at each level, which were all processed independently. According to the study procedure, two sets of results were obtained for each subject per level, as the same measurements were performed on both devices. Consequently, the same processing steps were carried out for the data from both devices in order to be able to compare them with each other.

At the strabismus level, the vertical and horizontal differences between the fixed and movable stimuli were stored for each individual measurement. This results in either two or four horizontal and vertical values for each direction of gaze. To obtain the average deviation for each azimuth, the horizontal and vertical mean was calculated from these values. From these mean deviations, the length of the shift vector at each azimuth was calculated with  $\sqrt{h^2 + v^2}$  ( $h$  indicates the horizontal shift and  $v$  the vertical shift). At the suppression level, two MCT values and two contrast values were stored per subject. These values were used unprocessed for further analysis. At the stereopsis level, it was stored for each run, which disparity the balls had, how long it took for a ball to be touched and whether the correct ball was hit. From this, the number of balls correctly played per disparity was stored for each subject, and additionally, all reaction times of misplayed balls were marked as not available. The evaluation refers exclusively to the reaction times of the correctly touched balls because the runs in which no ball was touched are also counted as misplayed balls. The measured times of the non-touched balls are larger than those of the touched balls, because the time is first stopped when the balls disappear again. For this reason, the times of the non-touched balls would falsify the reaction times.

Furthermore, significances between the datasets of the Vive Pro and the Vive Focus Plus were calculated in each comparison. Therefore, the Shapiro-Wilk test was first carried out, to check

whether the data is normally distributed or not. Based on the Shapiro-Wilk, the significance was determined by using the Wilcoxon signed rank test. In addition, the results of the questionnaires were tested for significance as well and the SuS score was calculated according to Brokk [Bro96]. Finally, the Spearman correlation between the answers to question 4 of the IPQ and the results of the stereopsis level was performed, as well as the correlation between question 4 and question 8 of the IPQ.

# Chapter 5

## Results

Presenting the results of the conducted study, this chapter is divided into three parts. First, the outcomes of the visual acuity measurements are shown. The second part refers to the results of the individual levels of the VR-Amblyopia Trainer described in chapter 4.2. And at the end, the answers to the two questionnaires, the Sus and the IPQ, are presented. The results of the two devices are compared with each other by using boxplots.

### 5.1 Visual Acuity

Figure 5.1 compares the visual acuities determined for each subject. The individual values are divided into two groups according to the device used after each measurement. The distributions of the achieved visual acuities do not differ significantly between both datasets. Accordingly, the mean of the Vive Focus Plus ( $1.47 \pm 0.29$  VAdec) and the Vive Pro ( $1.45 \pm 0.26$  VAdec) are very similar.

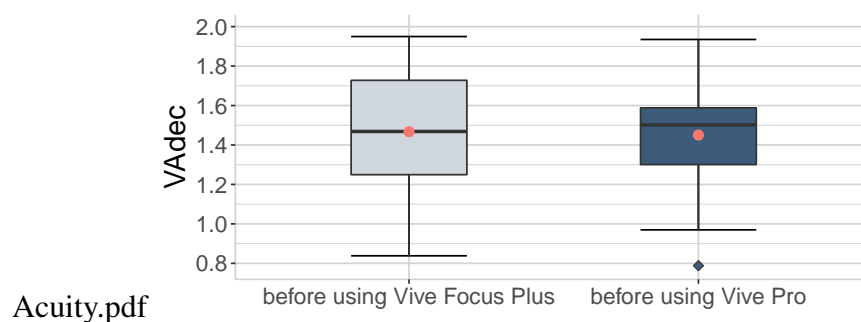


Figure 5.1: **Visual Acuity.** The plot shows the distribution of the visual acuities, measured before the corresponding device was tested.

## 5.2 VR-Amblyopia Trainer Results

This subsection divides the results from the VR-Amblyopia Trainer into the individual levels. According to the order in the study, the measurements of the strabismus level are presented first, followed by the values of the suppression level and finally by the outcomes of the stereopsis level.

### 5.2.1 Strabismus Level

The results of the strabismus measurement are compared in three different ways. First, the vertical and horizontal shifts are plotted separately for each direction of gaze. Second, all horizontal and vertical shifts are compared regardless of their azimuth and finally, the vector lengths of all azimuths are plotted.

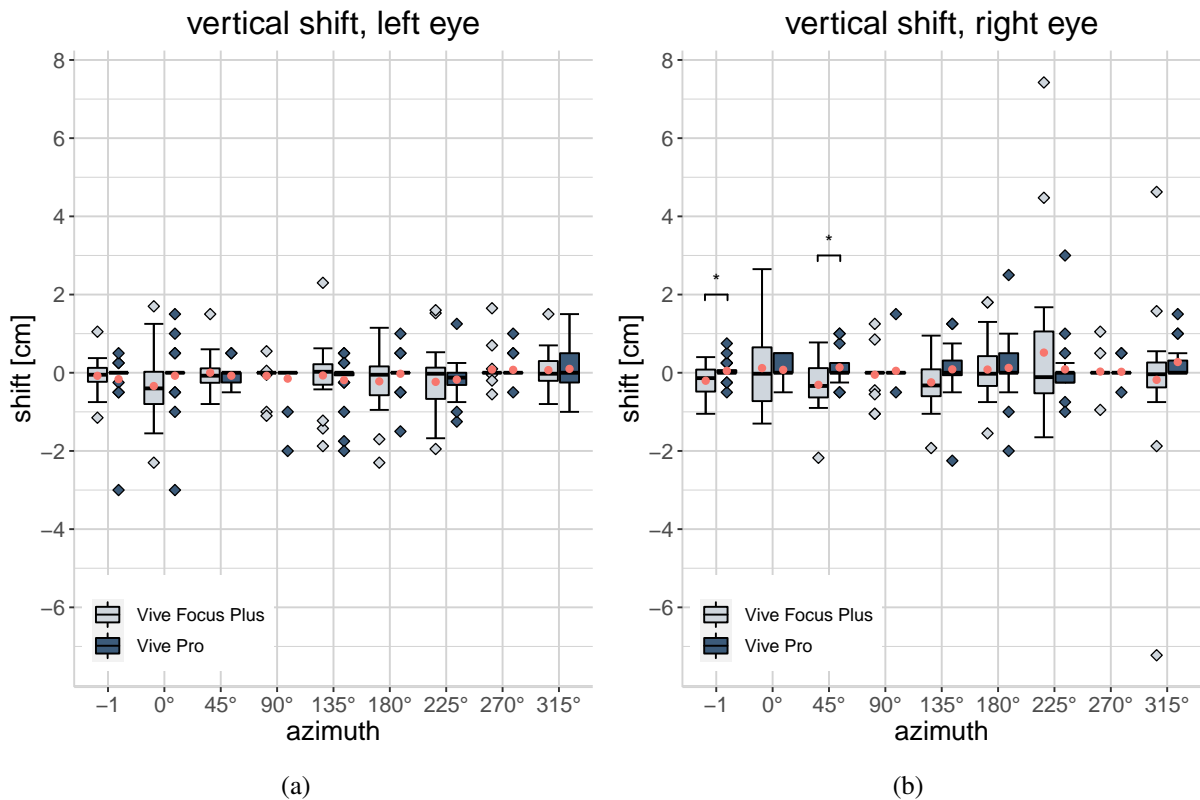


Figure 5.2: **Vertical shift in each azimuth.** Both plots show the distributions of the vertical shifts at each azimuth individually for the left and the right eye. The red points represent the mean of the respective dataset. In the left eye, an outlier of the Vive Focus Plus is cut out visually at azimuth 0° with  $y=15.3$  cm. (\* $p<0.05$ )

Figure 5.2 compares the vertical shifts for each device in the nine directions of gaze, divided into left and right eye. It shows that the interquartile range is 0 cm for both devices in azimuth  $0^\circ$  and  $270^\circ$ . At all remaining directions of gaze, except for azimuth  $315^\circ$  of the left eye, the interquartile ranges of the Vive Focus Plus are larger than those of the Vive Pro. However, Q1 and Q2 are always within the range of -1 cm to 1 cm, except for the Q2 at azimuth  $225^\circ$  in Figure 5.2(b). Furthermore, according to the Wilcoxon signed rank test, it exist two significant differences between the two devices at azimuth -1 ( $p < 0.05$ ,  $r = 0.46$ ) and azimuth  $45^\circ$  ( $p < 0.05$ ,  $r = 0.443$ ) in Figure 5.2(b) ( $p < 0.05$ ). At this azimuth, however, all values are within the range of -1 cm to +1 cm except for one outlier at -2.2 cm from the Vive Focus Plus.

Complementary, Figure 5.3 illustrates the horizontal shifts for each device in each direction of gaze. It is noticeable that the mean values of the Vive Focus Plus are smaller than the mean values of the Vive Pro in every azimuth. Additionally, all medians of the Vive Pro are negative, except for azimuth  $135^\circ$  in the left eye. The largest difference between the medians is in Figure 5.3(a)

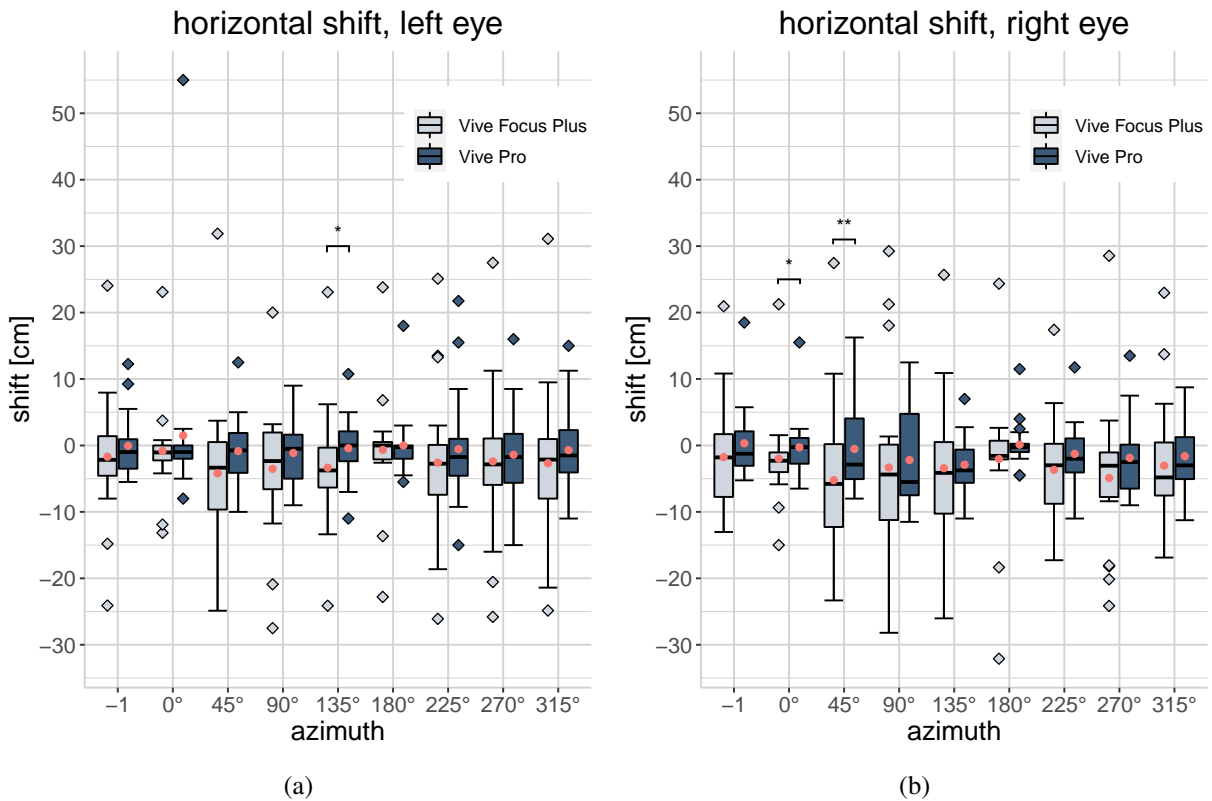


Figure 5.3: **Horizontal shifts in each azimuth.** Both plots show the distributions of the horizontal shifts at each azimuth individually for the left and the right eye. The red points represent the mean of the respective dataset. (\* $p < 0.05$ , \*\* $p < 0.01$ )

at azimuth  $135^\circ$  with a difference of 3.8 cm. Accordingly, there exists a significant difference between the two datasets of the devices at this direction of gaze ( $p < 0.05$ ,  $r = 0.46$ ). In the right eye (Figure 5.3(b)) exists a significant difference at azimuth  $45^\circ$  ( $p < 0.05$ ,  $r = 0.59$ ), with a median difference of 2.9 cm and another significant difference at azimuth  $0^\circ$  ( $p < 0.01$ ,  $r = 0.48$ ) with a difference of 2.1 cm. Furthermore, in both eyes, the interquartile ranges of both devices at azimuth  $0^\circ$  and  $180^\circ$  are smaller compared to all other interquartile ranges.

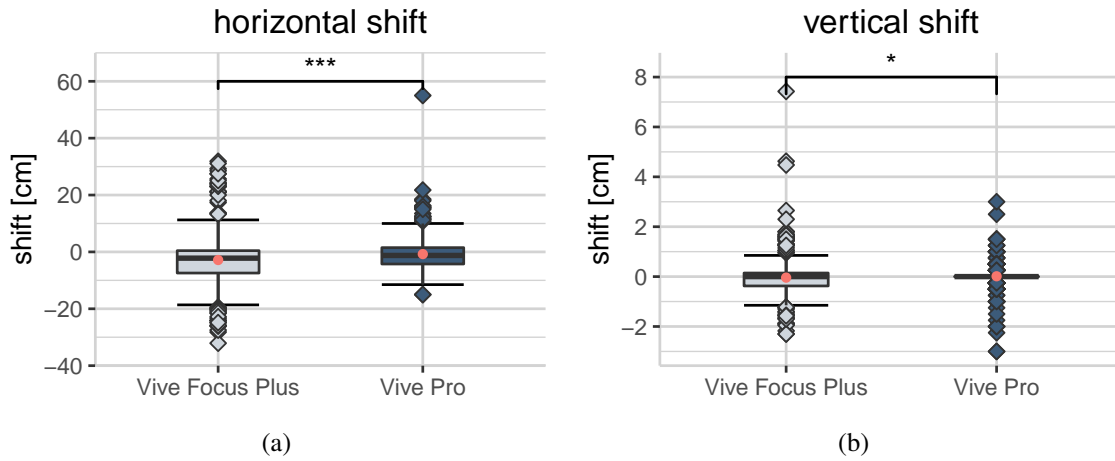


Figure 5.4: **Horizontal and vertical shift.** The distributions of all horizontal shifts and all vertical shifts are shown independent of the azimuth. The red points indicate the mean of the respective dataset. In the vertical shifts, two outliers at  $y = 15.3$  cm and  $y = -7.2$  cm of the Vive Focus Plus are cut out visually. (\*\* $p < 0.01$ , \*\*\* $p < 0.001$ )

In Figure 5.4 the values are divided into horizontal and vertical shifts, but independent of their azimuth. For both horizontal and vertical displacements, Q2 and the mean value of the Vive Focus Plus are below the corresponding values of the Vive Pro. The mean and standard deviation of the Vive Focus Plus are  $(-2.85 \pm 10)$  cm for the horizontal shifts and  $(-0.02 \pm 1.24)$  cm for the vertical shifts, while for the Vive Pro they are  $(-0.77 \pm 6.15)$  cm (horizontal shifts) and  $(-0.01 \pm 0.55)$  cm (vertical shifts). Furthermore, the interquartile range of the Vive Focus Plus is again larger than that of the Vive Pro in both cases and there is a significant difference in Figure 5.4(a) ( $p < 0.001$ ,  $r = 0.30$ ) as well as in Figure 5.4(b) ( $p < 0.05$ ,  $r = 0.11$ ).

Finally, the length of the resulting vector was calculated from the horizontal and vertical shift at each direction of gaze. Figure 5.5 shows that the values of the Vive Focus Plus are larger and shifted further upwards than the values of the Vive Pro. While the mean and standard deviation of the Vive Pro are  $(4.28 \pm 4.51)$  cm, they are  $(7.29 \pm 7.5)$  cm for the Vive Focus Plus. Q2 of the Vive Focus Plus is 10.31 cm, which is 4.77 cm higher than Q2 of the Vive Pro. Accordingly, there is a significant difference between the datasets of both devices ( $p < 0.001$ ,  $r = 0.41$ ).

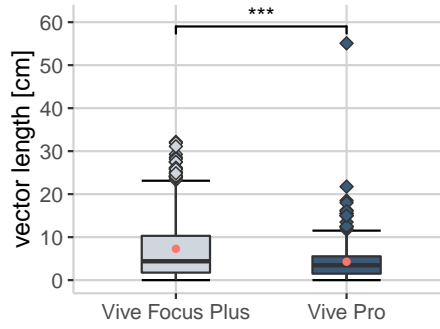


Figure 5.5: **Vector length.** The plot contains all vector lengths for each subject at each direction of gaze calculated with  $\sqrt{h^2 + v^2}$  (h indicates the horizontal shift and v the vertical shift). The red points indicate the mean of the respective dataset. (\*\*\*) $p < 0.001$

### 5.2.2 Suppression Level

The results from the suppression level are shown in Figure 5.6 in two different plots, one including the MCT values and one containing the contrast values. The results of the MCT tool are shown individually for the two VR devices in Figure 5.6(a). The Wilcoxon signed rank test does not yield any significant differences between the two datasets. All obtained values are among 40 % for both devices with one exception for the Vive Pro. However, the interquartile range of the Vive Focus Plus data is smaller, resulting in both the mean and Q2 being lower than those of the Vive Pro. Accordingly, the mean and standard deviation of the Vive Focus Plus ( $22.84 \pm 8.37$  %) are smaller than of the Vive Pro ( $26.15 \pm 13.15$  %).

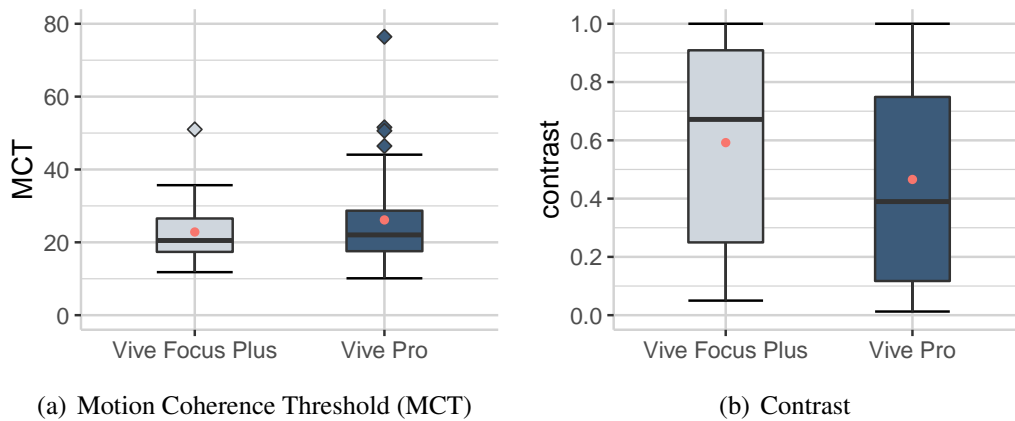


Figure 5.6: **Suppression results.** Both plots contain two values of each subject. (a) represents the distribution of the MCT and (b) the reached contrasts. The red points represent the mean of the respective dataset.

Figure 5.6(b) shows the distribution of the contrast values. It exists no significant differences between the two datasets, but the distributions of the values of both devices are among each other not as similar as the distributions of the MCT. On average the mean values of the Vive Focus Plus ( $0.59 \pm 0.35$ ) are larger than those of the Vive Pro ( $0.47 \pm 0.35$ ). Consequently are Q1 and Q2 of the Vive Focus Plus located at 0.25 and 0.91, while Q1 and Q2 of the Vive Pro are shifted downward (Q1=0.12, Q2=0.75).

### 5.2.3 Stereopsis Level

Figure 5.7(a) contains all reaction times that were needed until the correct ball was played in the stereopsis level, ignoring the times of the wrong reactions. Figure 5.7(b) shows how many balls per disparity and subject were played correctly. As a reminder, a total of 48 runs were performed, in which each disparity occurred 16 times. Accordingly, a maximum of 16 correct balls can be touched per disparity.

The reaction time using the Vive Focus Plus is significantly longer than using the Vive Pro for disparity 275 ( $p < 0.001$ ,  $r = 0.67$ ), disparity 550 ( $p < 0.001$ ,  $r = 0.67$ ) and disparity 825 ( $p < 0.001$ ,  $r = 0.68$ ). The medians of both devices differ from the smallest to the largest disparity by 42.44 ms, 44.01 ms and 44.06 ms. Furthermore, within the Vive Pro dataset, the median speeds up by almost 10 ms between disparities 275 to 550 and then by another 5 ms at disparity 825. In contrast, the median of the Vive Focus Plus decreases by only 1 ms with each larger disparity.

While there was little to no difference in response time between disparities, there is a strong change between disparities in Figure 5.7(b), especially for the Vive Focus Plus. In contrast to the Vive Pro, where the median is already 15 at the smallest disparity and 16 at the next larger one, the Vive Focus Plus starts with a median of 14, which then increases by one with each disparity. Even greater differences between the devices are seen in the interquartile ranges and the positions of Q1 and Q2. In all three disparities, Q1 of the Vive Pro and Q2 of the Vive Focus Plus are at nearly the same height. Accordingly, Q1 of the Vive Focus Plus is further down. The biggest difference exists in the smallest disparity, where Q1 of the Vive Focus Plus is located at 12. In disparity 550 it is located at 14, and in the largest disparity at 15. According to the different distributions, the Wilcoxon signed rank test yields a significant difference at disparity 275 ( $p < 0.05$ ,  $r = 0.55$ ) and 550 ( $p < 0.05$ ,  $r = 0.59$ ). Only for the largest disparity exists no significant difference.



### 5.3 SuS and IPQ

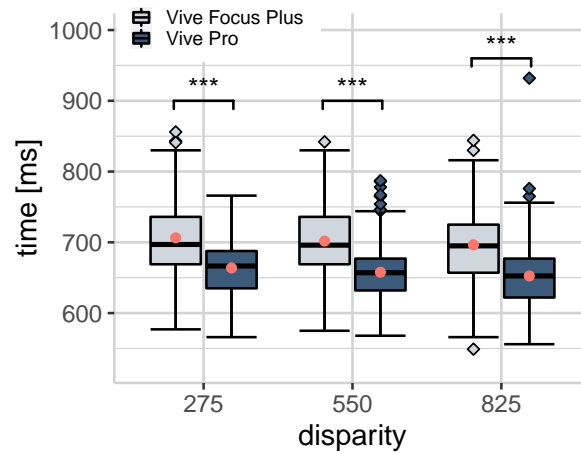
The comparison of the answers for each question of the SuS can be seen in Figure 5.8(a). In the SuS, there were five possible answers per question, which ranged from one (“strongly disagree”) to five (“strongly agree”). The Wilcoxon signed rank test did not reveal a significant difference between the answers regarding the two devices for any of the questions. Furthermore, for all but two of the questions, the interquartile ranges of the responses are similar between both devices. Accordingly, the SuS scores of both devices are similar with a score of 87 for the Vive Focus Plus and 85.88 for the Vive Pro.

In the IPQ, presented in Figure 5.8(b) an answer option between one and seven could be selected for each question. The wording of the answers varies between the questions but basically, seven always stands for agreement and one for disagreement. The only significant difference between the answers for both devices is determined in question 4 (“I did not feel present in the virtual space.”). While the median of both datasets with answer five is identical, the overall distribution of answers regarding the Vive Focus Plus is distributed towards “fully disagree”, and the answers regarding the Vive Pro towards “fully agree”. In addition to question 4, the answers to question 8 (“I was not aware of my real environment.”) are not very evenly distributed between the devices as well, although the difference is not yet significant according to the Wilcoxon signed rank test. The answers to question 8 are distributed towards “fully agree” for the Vive Focus Plus and towards “fully disagree” for the Vive Pro. To check whether the answers to questions 4 and 8 were related, Spearman correlation was performed. The Spearman correlation coefficients are listed in Table 5.1. These outcomes result in a non-significant small negative correlation for both the Vive Pro and Vive Focus Plus responses.

Due to the significant difference in question 4 of the IPQ, a Spearman correlation between the answers in question 4 and the results of the stereopsis level was additionally performed. However, the correlation did not reveal significant relationships between the questionnaire responses and the stereopsis level results for any of the devices, as shown in Table 5.1. The results of the correlation coefficients are not particularly meaningful, since the values are quite small and there is also no significance. However, it can be seen that there is a negative correlation for the reaction time and the number of correct balls of all disparities for the Vive Pro and a positive correlation for the Vive Focus Plus.

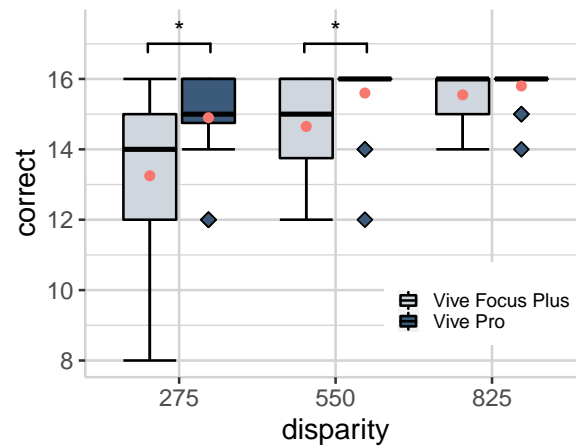
		Reaction time (mean)		Correct (total)		Question 8	
		Pro	Focus	Pro	Focus	Pro	Focus
Question 4	Pro	$r_s = -0.215$	-	$r_s = -0.164$	-	$r_s = -0.06$	-
		$p = 0.363$	-	$p = 0.49$	-	$p = 0.8$	-
	Focus	-	$r_s = 0.155$	-	$r_s = 0.138$	-	$r_s = -0.154$
		-	$p = 0.513$	-	$p = 0.562$	-	$p = 0.518$

Table 5.1: The Table presents the correlations between the answers to question 4 of the IPQ and the results of the stereopsis level as well as the answers to question 8 of the IPQ. For the reaction time, the mean of all three disparities was chosen as the comparative value per subject, and for the number of correct balls, the sum of all disparities per subject was used. The Spearman correlation coefficients  $r_s$  and the associated significance levels  $p$  are presented.



- Time per Disparity.pdf

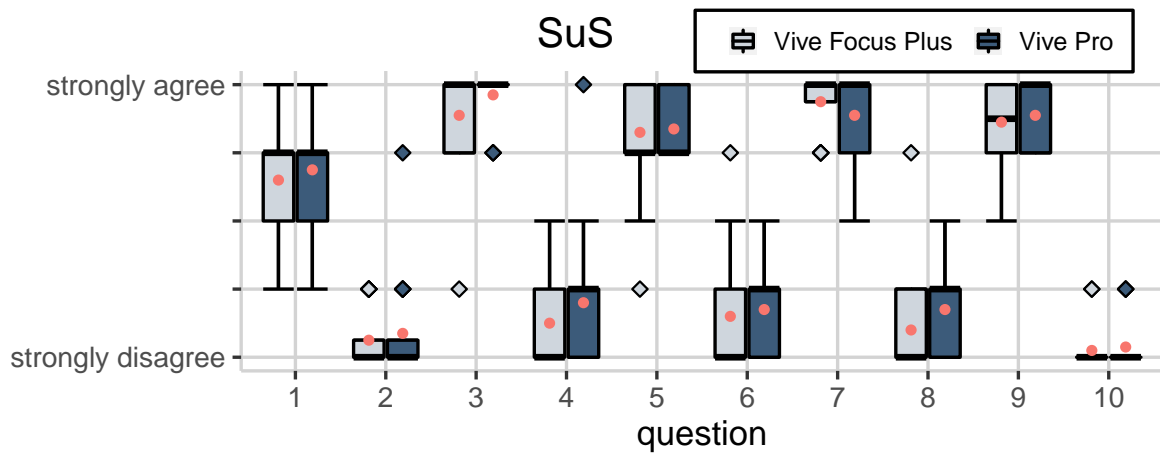
(a) Reaction time per disparity



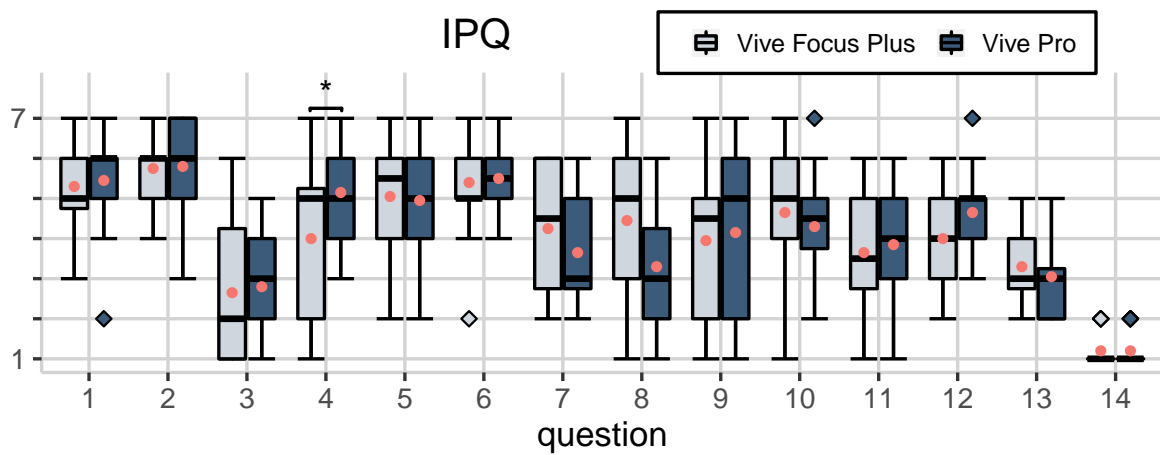
- Correct per Disparity.pdf

(b) Correct per disparity

Figure 5.7: **Stereopsis results.** (a) shows the distributions of the number of correct reactions per subject in each disparity. (b) shows for each disparity the distributions of the reaction times needed until a correct ball was hit. The red points represent the mean of the respective dataset and the significances between each disparity were calculated using the Wilcoxon signed rank test. (\* $p < 0.05$ , \*\*\* $p < 0.001$ )



(a) System Usability Scale



(b) Igroup Presence Questionnaire

Figure 5.8: **SuS and IPQ.** (a) shows the distribution of the answers from the SuS and (b) the answers of the IPQ. The red points represent the mean of each dataset and the significances of each question were calculated using the Wilcoxon signed rank test. (\* $p < 0.05$ )

# Chapter 6

## Discussion

The conducted study aimed to determine whether the modified VR-Amblyopia Trainer is capable of delivering comparable results on the standalone device to those achieved on the Vive Pro. For this purpose, 20 subjects tested the VR-Amblyopia Trainer on both devices. Since the study is primarily concerned with the comparison of the software of the VR-Amblyopia Trainer, two points regarding the hardware and software of the HMDs are anticipated here in advance. The resolution of both devices should be identical, as both have a 3.5" display with the same number of pixels. However, the Vive Pro has a higher refresh rate of 90 Hz, which means that more images are calculated per second and thus possibly a smoother image is created. The following discussion is about whether the results of both devices are comparable based on visual acuity and afterward whether the software modifications described in chapter 4.3 were sufficient to achieve comparable results on both devices despite the differences in the HMDs.

### 6.1 Visual Acuity

The visual acuity of each subject was measured before each run for two reasons. On the one hand, this was to exclude the possibility that subjects with low visual acuity would have problems solving the tasks due to poor vision. The second reason is particularly important in relation to the comparability of all results in the study. The second measurement should rule out any significant change in visual acuity between the first and second run, since poorer visual acuity could already be a reason for worse results in the VR-Amblyopia Trainer. In order to obtain highly reliable results with the Fract test and to be able to compare them between the two runs, the test was performed three times for each eye, since according to Michael Bach the measurement must be conducted more than once to obtain a stable visual acuity value [Bac06]. Because the values

of the study are probably quite credible due to the triple measurement, reliable statements can be made based on the distributions shown in Figure 5.1. As there are no significant differences between the two datasets of the measurements before each device and, besides, the mean values of both datasets are identical at about 1.5 VAdec, it can be assumed that differences in the results of the VR-Amblyopia Trainer are not because the visual acuities fluctuated between the runs.

## 6.2 Strabismus Level

When analyzing measurements from the strabismus level, it should be noted that the results of both devices can only be compared with each other to a limited extent, since only integers were determined for the Vive Pro while the Five Focus Plus measured with an accuracy of one decimal digit. There are nevertheless values depicted in between two integers for the Vive Pro in the graphs of chapter 5.2.1, since the mean value was calculated from the measurements at one azimuth to obtain one horizontal and one vertical shift in each azimuth. Because of the different measurement accuracies, no reliable statement about relations can be made from differences smaller than 2 cm.

When looking at the vertical shifts in Figure 5.2, it is particularly noticeable that most of the values of both devices are located between -1 cm and 1 cm. However, the interquartile ranges of the Vive Focus Plus are always larger than those of the Vive Pro with one exception. These smaller values of the Vive Pro could be related to the different measurement accuracies of the two devices. It is possible that the program on the Vive Pro has cut off the decimal places of the measured values to obtain integers, which leads to smaller amounts. Accordingly, with the same measurement of 0.9 cm, the Vive Pro would have stored 0 cm, while the Vive Focus Plus stored 0.9 cm. This assumption is supported by the fact that apart from two azimuths in the right eye, no significant differences were measured in the individual azimuths, despite the inaccurate values of the Vive Pro. Accordingly, it can at least be assumed that the measurements in the vertical direction mostly differ by only 1 cm.

In the distribution of the horizontal shift values, it is particularly striking that all medians of the Vive Pro are negative with only one exception. Additionally, it should be noted that all of the mean values of the Vive Focus Plus are smaller than those of the Vive Pro. Thus, since the median values are mostly in the same sign range and the amounts of the median values of the Vive Focus Plus are again larger than those of the Vive Pro, the difference may as well be related to the different measurement accuracies.

However, in contrast to the vertical shifts, the values of the horizontal shifts are much larger for both devices and besides, the outliers of the Vive Focus Plus are larger than those of the Vive Pro.

Nevertheless, significant differences occur at only two azimuths per eye, but if, in addition to the individual gaze directions, all vector lengths and horizontal and vertical shifts are considered independently of their azimuth, strong significances appear. These differences are not necessarily due to the different measurement scales of both devices, since the values of the Vive Focus Plus are sometimes much larger than those of the Vive Pro, especially in the horizontal shifts and do not only differ by  $\pm 2$  cm. This suggests that there are larger shifts on the Vive Focus Plus than on the Vive Pro. Since each subject tested each device in the study, it can be ruled out that this difference occurs due to undetected latent strabismus, as it would otherwise have occurred equally in both devices.

One possible explanation for variations in results between devices could be the panum's fusional area. As soon as the brain fuses the images of both eyes, the images appear perfectly superimposed and further movements within the panum's fusional area do not change the perception. Although the influence of the panum's fusional area is supposed to be eliminated by the measurements of the four directions, the subjects did not receive any information about the panum's fusional area. Therefore, the subjects may have shifted the stimulus within the panum's fusional area even further. Since this shift is no longer visually perceptible, it is possible that different results were obtained for one subject. To ensure comparability of both devices despite the panum's fusional area, subjects in further studies should be encouraged to confirm fusion immediately after it appeared. Thus, all repeated measurements on the same subject should result in the same limits of the panum's fusional range. The method used for measuring strabismus has already been investigated by Mehringer et al. [Meh20] in a study with 14 healthy subjects on the Vive Pro. A nasalward fusion range of  $25.8 \pm 13.6$  (mean  $\pm$  standard deviation) and  $27.5 \pm 16.9$  was determined. These large fusion ranges support the assumption that the panum's fusional area produced different results on the two devices. Another possible reason for the different results may be due to the foveated rendering on the Five Focus Plus, which is described in chapter 4.3. Since the feature makes the edges of the field of view less sharp, it is possible that it made it harder to tell when the two images were fused, as it could appear slightly blurry even with a perfect overlap. In a paper, Albert et al. named eye tracking as an important prerequisite for the use of foveated rendering, since otherwise everything can only be perceived sharply with the help of head movement, which does not correspond to reality. With eye tracking, the area of high resolution would therefore not be fixed in the center of the lens, but the area of the viewing direction would always be displayed in high resolution [Alb17]. Since the Vive Focus Plus is not capable of eye tracking, the foveated rendering function seems to be disadvantageous especially in the strabismus level, where only with the help of eye movements the stimuli can be perceived.

### 6.3 Suppression Level

The measurements at the suppression level provided good results, as no significant differences occurred in either of the two measurements. Especially in the MCT measurement, the distributions of both datasets are very similar. Furthermore, the median values of 22.0 % for the Vive Pro and 20.5 % for the Vive Focus Plus are very close to the 20 % that speak for very good performance according to Ward et al. [War18]. The results of the contrast measurement are not quite as similar. Although there is no significance, the distributions of the values in Figure 5.6(b) show that greater contrasts were achieved with the Vive Focus Plus than with the Vive Pro. However, variations between the results of individual subjects are not necessarily due to performance. Liu et al. describes in a paper that stronger attention also increases the ability to recognize appearance of motion coherence [Liu06]. This allows for the possibility that differences occurred due to lack of interest and not due to the performance of an device. The study was mainly about the comparison of the software, but the worse results with the Vive Pro could also be related to the fact that the controllers sometimes did not take over the correct directional inputs on the trackpad. This assumption is based on statements made by the subjects during the study. This could have caused the measurement to end even though the subjects had not yet reached their possible maximum contrast. Overall, it can be concluded from the non-existent significant values that the suppression level was probably best adapted to the new device in terms of software technology and delivers the best and most satisfactory results in comparative terms.

### 6.4 Stereopsis Level

The most significant differences between the devices occurred at the stereopsis level. For both, the number of correct balls and the reaction time, the results of the Vive Pro were consistently better than those of the Vive Focus Plus. Better, in this case, means that more balls are played correctly and the reaction time is smaller.

However, the possible reaction time to touch a correct ball is limited due to the given circumstances. Firstly, the ball can only be touched until it passes the player. Secondly, it always takes some time before the ball can be touched at the earliest, as it has to fly towards the user from a distance of 2.14 meters and the user does not move freely in space. However, the reaction time can be shortened individually by leaning forward and stretching the arm to touch the ball earlier. Accordingly, it is expected that with a greater disparity, it is easier to recognize the correct ball and thus to touch it faster. This expected behavior can only be seen in the results of the Vive Pro, where the average reaction times change first by 10 ms and then by 5 ms from the smallest, thus



most difficult, disparity to the largest. With the Vive Focus Plus, on the other hand, the reaction time between the disparities practically does not change. In addition, with the Vive Pro, only one ball per subject was played incorrectly on average in disparity 275, and in the other disparities the medians and means are around 16, which means that all balls were played correctly. In contrast, subjects using the Vive Focus Plus were only able to play an average of 13 to 14 balls correctly in disparity 275, and even in the larger disparities, the distribution of balls played correctly is not completely on full score. Although it can undoubtedly be seen that the number of correct answers increases with increasing disparity, the scores of the Vive Focus Plus are nevertheless not as good as those of the Vive Pro in any of the disparities.

Based on the good results achieved with the Vive Pro, it can be assumed that all subjects were able to detect the front ball in all disparities. Since the results of the Vive Focus Plus were achieved by exactly the same subjects, it can be suspected that the worse results are due to worse performance of the Vive Focus Plus and not due to worse stereoscopic vision of the subjects. However, it should be noted that it is also possible that more balls were detected correctly, but they could not be touched in time with the Vive Focus Plus. Therefore, it is important to note that the reaction time not only involves recognizing which of the two balls is further forward but then moving the racket into the position where it can touch the correct ball. Since the average reaction time for the easiest and most difficult disparity is the same and does not change as expected, it can be assumed that this reaction time is possibly the last point at which the balls can be touched before they fly past the subject. Accordingly, it could be the case that more balls were recognized correctly than were touched since there was not enough time left to bring the racket into the correct position. But with larger disparities, it was recognized faster which ball had to be played and the remaining time was then sufficient to bring the racket into position.

Nevertheless, the significant differences between the two devices, both in reaction times and in the number of correct balls, indicate that the stereopsis level on the Vive Focus Plus does not work as well and smoothly as on the Vive Pro. This means that the modifications made were not adapted strongly enough to the lower frame rate and processing power of the Vive Focus Plus.

One way to reduce the processing power could be to reduce the environment of the stereopsis level to a minimum. This means that the user would be surrounded by nothing but white, only seeing the balls and controllers. However, since the used materials are already very simple, and the objects do not make any movements, it is improbable whether this would improve performance. For this reason, it is necessary to consider adapting the entire task. Trying to stay as close as possible to the original task, the movement of the controllers could be eliminated. As a replacement, the controllers could be used to indicate on the trackpad whether the right or left ball

is further forward. This way, it would not be necessary to calculate per tick where the controller is located and whether there was contact between the controller and one ball.

A study by Díaz et al. compared a low cost VR device to a higher quality and higher cost VR device in terms of experience and knowledge gain. The higher cost VR device is considered to be of higher quality due to a higher refresh rate. The outcomes of the study show that both devices support spatial and experimental learning in a similar way. The only difference occurred in terms of the time needed to complete the tasks. The time needed by the the low cost device was significantly higher than the time of the other device [Día19]. Taking into account the results of this study, another way to adapt the stereopsis level to the Vive Focus Plus could be to increase the distance between the user and the place where the balls appear. In this way, the extended flight time could provide the opportunity to touch the correct ball despite poorer performance. However, it is possible that a longer decision time would simultaneously lower the difficulty level, which could possibly reduce learning effects.

## 6.5 SuS and IPQ

The subjective perception of each subject regarding usability and the sense of presence in the VR was measured after each device with two questionnaires. The primary goal of the study was the comparison of the software and not the hardware. For this reason, the subjects were located in the main menu directly after putting on the headset and did not have to start anything themselves, which resulted in an identical process for both devices. And since the modifications made to the VR-Amblyopia Trainer affect performance rather than gameplay itself, it was assumed that the results of the SuS would not differ between the two devices. This assumption is supported by the distributions of the answers, as there were no significant differences between the devices in any of the questions. In addition, the SuS scores of both devices differ only minimally from each other and are both within the range of excellent usability, which is defined by a score of  $>85$  according to Bangor et al. [Ban08].

In addition to usability, the IPQ was filled out by each subject. There were no significant differences in the answers to this questionnaire, except for one question. However, the significant difference in question 4 could lead to the conclusion that the subjects felt more present in the VR when using the Vive Focus Plus than by using the Vive Pro. This assumption is strengthened by the answers to question 8 since the results of this question are not yet significant but optically nevertheless very distributed. The correlation of the answers to question 4 and question 8 confirms a connection of these but only not significant and with a small correlation. This difference in

sense of presence between the devices could be due to different performances of the devices. However, this would also lead to the conclusion that the results of the Vive Focus Plus should be better than those of the Vive Pro. But this assumption is refuted, especially by the results of the stereopsis level, where consistently better results were recorded for the Vive Pro. Accordingly, there exists no significant correlation between the answers to question 4 and the results of the stereopsis level. Various conclusions can be drawn from this. On the one hand, it is possible that the questions were answered rather thoughtlessly and disinterestedly, which is supported by the fact that no significant correlation can be demonstrated between the answers to the similar questions 4 and 8 either. However, it should also be noted that three different levels were played in the VR-Amblyopia Trainer, and the questionnaires referred to the entire application and at least in the suppression level, the results of the Vive Focus Plus were a bit better. Furthermore, the IPQ contains 14 questions, among which the answers to only one question differ significantly between the two devices. This could also lead to the conclusion that the sense of presence was pretty much the same for both devices.

The study by Díaz et al. already mentioned in chapter 6.4, additionally compared the user experience in terms of the perception of the sense of presence. The results for both devices were very similar, although there are obvious differences in the low cost device due to the significantly larger reaction times [Día19]. These results are similar to those from the study conducted in this work, as the VR-Amblyopia Trainer results showed very similar responses in terms of the sense of presence, although the reaction times of the Vive Pro were smaller than those of the Vive Focus Plus. This suggests that the sense of presence does not necessarily depends on the image quality and performance.



# Chapter 7

## Conclusion and Future Work

The goal of this thesis was to derive a version of the existing VR-Amblyopia Trainer, described in chapter 4.2, that can be used by patients independently at home. For this purpose, the application was modified and adapted to be used on the standalone device, the Vive Focus Plus. The modified version should be able to deliver comparable results to the version on the Vive Pro, despite the lower processing power of the Vive Focus Plus. To verify whether the standalone device is capable to achieve the same results, a study was conducted with healthy subjects. Each subject tested both devices and in chapter 5, the results of both devices were compared individually for each level. While the questionnaires to be answered referred to the entire VR-Amblyopia Trainer and thus give an impression of the entire application, the results of the measurements of the VR-Amblyopia Trainer provide information about the individual levels.

The responses to the questionnaires showed that the applications, neither in the ease of use nor in the sense of presence differ significantly. There was only one question that showed significance, but this was not supported by any correlations. However, the results of the measurements showed that the individual levels of the application were adapted differently well to the new device.

The best results were obtained for the suppression level, where no significant differences exist and the mean values of both devices are within the range of normal values for healthy subjects. Accordingly, the changes made at this level seem to be just right to enable a good game flow on the Vive Focus Plus. The strabismus level, on the other hand, delivers slightly different results between the devices. In order to improve especially the horizontal results of the Vive Focus Plus to achieve more precise measurements, the foveated rendering at this level could be removed to check whether it is easier to recognize when the images are superimposed. However, it should be noted that the performance of the level could get worse, since foveated rendering saves computing power. This would require testing whether the measurement can be improved by removing the foveated

rendering, without degrading performance to a point where the stability of the measurement is again compromised. Furthermore, in a new study, it would be advisable to tell the subjects to confirm immediately after the two images have been fused. This ensures that the results actually reflect the boundaries and not random points within the panum's fusional area. Especially with a similar study design in which the same subjects test both devices, the same results should be obtained for the boundaries of the panum's fusional areas. At least as far as the devices can actually measure comparable data. The worst results were achieved in the stereopsis level. Neither in the number of correct balls nor in the reaction times could comparable results be achieved. It can be concluded that the performance in this level on the Vive Focus Plus is not sufficient to solve the given task reasonably. It may be due to the fact that the necessary calculations for the execution of the level are too extensive to be implemented in such a way that, in addition to the flying balls, the racket can be moved in time as well. Better results could possibly be achieved by no longer having to touch the correct ball with the racket, but by simply indicating on the trackpad whether the right or left ball is further forward. This could increase the number of correct balls a bit, but presumably, the performance of the flying balls would still not come close to the performance of the Vive Pro. Furthermore, the stereopsis level could be changed to a more passive training method, with as little movement as possible. For example, several objects could simply be positioned in the room, between which the object has to be determined that is further forward. However, both variations of the stereopsis level reduce the direct interactivity of the application, which could lead to a more rapid loss of interest in the game and thus to less success in amblyopia therapy.

In summary, the VR-Amblyopia Trainer on the Vive Focus Plus currently only works for functions that do not require time-dependent reactions. However, since the stereopsis level works smoothly on the Vive Focus Plus, it seems to be possible to achieve reasonable results and game flows on the new device. Accordingly, further improvement of the performance should be aimed at, but taking into account that further adjustments mean a balancing act between stable measurements and good performance.

# Appendix A

## Patents

### A.1 Method and apparatus for the treatment of amblyopia

**Publication Number:** US9597253B2

**Date of Publication:** Mar. 21, 2017

**Inventors:** Sascha Seewald, Nicolaus Widera

**Assignee:** Caterna Vision GmbH

**Abstract:** A method for the treatment of amblyopia comprising the steps of diagnosis and approval of a patient by a medical practitioner, providing access to an eye-training platform for the approved patient and instructions to the approved patient on using the eye-training platform, preparation of a therapy protocol by the medical practitioner, use of the eye-training platform according to the therapy protocol, recordal of patient results, intermediate examination of the patient and review of patient results, further use of the eye-training platform according to a modified therapy protocol, recordal of further user results, and examination of visual acuity and review of user results by the medical practitioner.

## A.2 Interactive system for vision assesment and correction

**Publication Number:** US9706910B1

**Date of Publication:** Jul.18, 2017

**Inventors:** James J. Blaha, Manish Gupta

**Assignee:** Vivid Vision, Inc.

**Abstract:** Systems and methods for assessing vision and correcting vision problems are provided. A head-mountable virtual reality display controlled via a computing device can be worn by a user to display virtual reality images to the user. The images can be displayed as part of an interactive and engaging activity that can be used to determine a value of a certain parameter of the user's eyes. The activity can also be intended as a treatment procedure during which user's eyes are trained to perceive objects having certain properties that unassisted eyes of the user are normally notable to perceive. User input is acquired to determine user's perception of the displayed virtual reality images. The computing device can be a Smartphone configured to perform the vision tests or treatment under control of a remote computing device operated by a trained clinician.



### **A.3 Method and apparatus for treating diplopia and convergence insufficiency disorder**

**Publication Number:** US 20190159956A1

**Date of Publication:** May 30 , 2019

**Inventors:** Joseph Koziak

**Abstract:** A method of treating diplopia or convergence insufficiency disorder in a patient; it includes providing a patient having a condition of diplopia or convergence insufficiency disorder with an image pair configured to present a first image to a first weaker eye of the patient and a second image to a second dominant eye of the patient; obtaining performance information of the patient when the patient performs a task requiring the perceiving of at least the information content of the first image; and adjusting, based on the performance information, the at least one image parameter such that the difference in perceptibility of the information content of the first image and the information content of the second image is reduced.



# List of Figures

2.1	<b>Structure of the human eye.</b> The anatomy of the human eye, including the elements mentioned in chapter 2.1, based on [Atc00]. . . . .	4
2.2	<b>Stereopsis in human eyes.</b> The star is focused with both eyes, whereby being imaged on the fovea. Due to the alignment of the eyes, the triangle falls with two different angles $\alpha$ and $\beta$ through the eyes at two non-corresponding points on the retinas. The distance between the triangle and the star can be calculated with the help of the projection points. Additionally, the dashed line illustrates the Empirical Horopter, which runs through the focused star. The yellow lines represent the boundaries of the panum's fusional area. Based on [Nit17, Wri06]. .	5
2.3	<b>Strabismus.</b> While the left eye focuses on the star, which is accordingly imaged on its fovea (F), the squinting eye is not aligned accordingly and the star is imaged on a non-corresponding point, based on [Wri06]. . . . .	7
2.4	(a) represents the state of a healthy eye in which the light is focused on the retina. In (b) and (c), however, the light is focused behind and before the retina, because of refraction errors, based on [Har19]. . . . .	8
3.1	The screenshot shows the structure of a game from Caterna. The black and white grid pattern in the background represents the stimulus, while the colored balloons in the foreground are used to perform certain tasks, based on Caterna Vision GmbH <sup>1</sup> . . . . .	14
4.1	<b>Main menu.</b> The different levels are represented with pictures on the wall. Below left the strabismus level, below right the suppression level and above the stereopsis level in three different environments. Each level can be selected by pointing the controller at the corresponding image and pressing a button. . . . .	21

- 4.2 **Strabismus stimulus.** (a) The stimulus consists of 4 identical balls arranged evenly around one cross. (b) Each stimulus is only visible in one eye. The green colored stimulus is displayed offset to the other, causing double images to be perceived. This stimulus can be moved in the four main directions. In the correct application, both stimuli have the same colors. (c) represents the designations for the nine different azimuths, in which the stimuli are displayed. . . . . 22
- 4.3 **Perception of stimuli with strabismus.** The stimulus not colored green corresponds to the stationary one and is only visible to the left eye. The left eye is aligned in a way that the stimulus is imaged on the fovea. The broken line going from the stationary stimulus through the fovea of the squinting eye is meant to represent how a healthy eye would be aligned. The green colored stimulus is the movable stimulus and can only be perceived by the right eye, the squinting eye. Although the stimulus is not in the same position as the other one, it is still imaged on the fovea due to the eye position. The angle  $\alpha$  between the broken and solid line corresponds to the squint angle of the eye. . . . . 23
- 4.4 **Suppression Stimulus.** It is illustrated what both eyes are shown during which tool. In (a), both eyes receive the same animation. In this example, there are one hundred points, 10 % of which (represented by red arrows) move to the right. In (b), a Motion Coherence Threshold of 10 is displayed to the right eye, which moves to the right. The left eye only receives the remaining points, randomly moving. Additionally, a contrast is added to the left eye. . . . . 25
- 4.5 **Stereopsis level.** The user is placed in front of a table. From the opposite side of the table, two balls fly towards the user at the same time. . . . . 27
- 4.6 **Foveated rendering.** The green rectangle represents the foveated region, where everything is shown very sharp and the size of the rectangle can be varied. The yellow area represents the peripheral region, whose resolution is lower and can be set to low, medium or high. Based on VIVE Wave<sup>6</sup>. . . . . 29
- 4.7 **Controller instruction.** The image for the stereopsis level is shown as an example for the instructions. The blue button must be pressed in the level to start the task. Based on Vive Wave<sup>7</sup>. . . . . 29
- 4.8 **Study design.** The study design for both groups is shown in the flow chart. Each group consisted of five female and five male subjects. The data recording procedure was the same for both devices and as questionnaires were filled out the SuS and the IPQ. . . . . 31

5.1	<b>Visual Acuity.</b> The plot shows the distribution of the visual acuities, measured before the corresponding device was tested. . . . .	35
5.2	<b>Vertical shift in each azimuth.</b> Both plots show the distributions of the vertical shifts at each azimuth individually for the left and the right eye. The red points represent the mean of the respective dataset. In the left eye, an outlier of the Vive Focus Plus is cut out visually at azimuth $0^\circ$ with $y=15.3$ cm. (* $p<0.05$ ) . .	36
5.3	<b>Horizontal shifts in each azimuth.</b> Both plots show the distributions of the horizontal shifts at each azimuth individually for the left and the right eye. The red points represent the mean of the respective dataset. (* $p<0.05$ , ** $p<0.01$ ) . .	37
5.4	<b>Horizontal and vertical shift.</b> The distributions of all horizontal shifts and all vertical shifts are shown independent of the azimuth. The red points indicate the mean of the respective dataset. In the vertical shifts, two outliers at $y=15.3$ cm and $y=-7.2$ cm of the Vive Focus Plus are cut out visually. (** $p<0.01$ , *** $p<0.001$ )	38
5.5	<b>Vector length.</b> The plot contains all vector lengths for each subject at each direction of gaze calculated with $\sqrt{h^2 + v^2}$ (h indicates the horizontal shift and v the vertical shift). The red points indicate the mean of the respective dataset. (** $p<0.001$ ) . . . . .	39
5.6	<b>Suppression results.</b> Both plots contain two values of each subject. (a) represents the distribution of the MCT and (b) the reached contrasts. The red points represent the mean of the respective dataset. . . . .	39
5.7	<b>Stereopsis results.</b> (a) shows the distributions of the number of correct reactions per subject in each disparity. (b) shows for each disparity the distributions of the reaction times needed until a correct ball was hit. The red points represent the mean of the respective dataset and the significances between each disparity were calculated using the Wilcoxon signed rank test. (* $p<0.05$ , *** $p<0.001$ ) . . . . .	41
5.8	<b>SuS and IPQ.</b> (a) shows the distribution of the answers from the SuS and (b) the answers of the IPQ. The red points represent the mean of each dataset and the significances of each question were calculated using the Wilcoxon signed rank test. (* $p<0.05$ ) . . . . .	42



# List of Tables

5.1 The Table presents the correlations between the answers to question 4 of the IPQ and the results of the stereopsis level as well as the answers to question 8 of the IPQ. For the reaction time, the mean of all three disparities was chosen as the comparative value per subject, and for the number of correct balls, the sum of all disparities per subject was used. The Spearman correlation coefficients  $r_s$  and the associated significance levels  $p$  are presented. . . . . 43





# Bibliography

- [Alb17] R. Albert, A. Patney, D. Luebke, and J. Kim. Latency requirements for foveated rendering in virtual reality. *ACM Transactions on Applied Perception*, 14(4):1–13, 2017.
- [Atc00] D. A. Atchison and G. Smith. *Optics of the human eye*. Butterworth-Heinemann, Oxford, 2 edition, 2000.
- [Bac06] M. Bach. The freiburg visual acuity test-variability unchanged by post-hoc re-analysis. *Graefe’s Archive for Clinical and Experimental Ophthalmology*, 245(7):965–971, 2006.
- [Ban08] A. Bangor, P. T. Kortum, and J. T. Miller. An empirical evaluation of the system usability scale. *International Journal of Human-Computer Interaction*, 24(6):574–594, 2008.
- [Bir13] E. E. Birch. Amblyopia and binocular vision. *Progress in Retinal and Eye Research*, 33:67–84, 2013.
- [Bro96] J. Brooke. *Sus: A quick and dirty usability scale*. In *Usability Evaluation in Industry*. Taylor & Francis, London, 1 edition, 1996.
- [Bui14] E. Bui Quoc and C. Milleret. Origins of strabismus and loss of binocular vision. *Frontiers in Integrative Neuroscience*, 8(71):1–19, 2014.
- [Cam78] F. W. Campbell, R. F. Hess, P. G. Watson, and R. Banks. Preliminary results of a physiologically based treatment of amblyopia. *The British journal of ophthalmology*, 62(11):748–755, 1978.
- [Día19] P. Díaz, T. Zarraonandía, M. Sánchez-Francisco, I. Aedo, and T. Onorati. Do low cost virtual reality devices support learning acquisition? a comparative study of two different vr devices. In *Proceedings of the XX International Conference on Human Computer Interaction*, pages 1–8, New York,NY,United States, 2019. Association for Computing Machinery.

- [Eas06] R. M. Eastgate, G. D. Griffiths, P. E. Waddingham, A. D. Moody, T. K. H. Butler, S. V. Cobb, I. F. Comaish, S. M. Haworth, R. M. Gregson, I. M. Ash, and S. M. Brown. Modified virtual reality technology for treatment of amblyopia. *Eye (London, England)*, 20(3):370–374, 2006.
- [Eco12] J. R. Economides, D. L. Adams, and J. C. Horton. Perception via the deviated eye in strabismus. *The Journal of neuroscience : the official journal of the Society for Neuroscience*, 32(30):10286–10295, 2012.
- [Fos17] A. J. Foss. Use of video games for the treatment of amblyopia. *Current opinion in ophthalmology*, 28(3):276–281, 2017.
- [Haa03] W. Haase. Amblyopien teil i: Diagnose. *Der Ophthalmologe*, 100(1):69–88, 2003.
- [Har19] E. N. Harb and C. F. Wildsoet. Origins of refractive errors: environmental and genetic factors. *Annual review of vision science*, 5:47–72, 2019.
- [Her16] N. Herbison, D. MacKeith, A. Vivian, J. Purdy, A. Fakis, I. M. Ash, S. V. Cobb, R. M. Eastgate, S. M. Haworth, R. M. Gregson, and A. J. Foss. Randomised controlled trial of video clips and interactive games to improve vision in children with amblyopia using the i-bit system. *British Journal of Ophthalmology*, 100(11):1511–1516, 2016.
- [Hes15] R. F. Hess and B. Thompson. Amblyopia and the binocular approach to its therapy. *Vision research*, 114:4–16, 2015.
- [Hol06] J. M. Holmes and M. P. Clarke. Amblyopia. *The Lancet*, 367(9519):1343–1351, 2006.
- [Hol11] J. M. Holmes, E. L. Lazar, B. M. Melia, W. F. Astle, L. R. Dagi, S. P. Donahue, M. G. Frazier, R. W. Hertle, M. X. Repka, G. E. Quinn, and K. K. Weise. Effect of age on response to amblyopia treatment in children. *Archives of ophthalmology (Chicago, Ill. : 1960)*, 129(11):1451–1457, 2011.
- [How95] I. P. Howard and B. J. Rogers. *Binocular vision and stereopsis*. Oxford University Press, New York, 1995.
- [Kel16] K. R. Kelly, R. M. Jost, L. Dao, C. L. Beauchamp, J. N. Leffler, and E. E. Birch. Binocular ipad game vs patching for treatment of amblyopia in children: a randomized clinical trial. *JAMA Ophthalmology*, 134(12):1402–1408, 2016.

- [Lev06] D. M. Levi. Visual processing in amblyopia: human studies. *Strabismus*, 14(1):11–19, 2006.
- [Liu06] T. Liu, S. Fuller, and M. Carrasco. Attention alters the appearance of motion coherence. *Psychonomic Bulletin & Review*, 13(6):1091–1096, 2006.
- [Meh20] W. A. Mehringer, M. G. Wirth, S. Gradl, L. S. Durner, M. Ring, A. F. Laudanski, B. Eskofier, and G. Michelson. An image-based method for measuring strabismus in virtual reality. In *2020 IEEE International Symposium on Mixed and Augmented Reality Adjunct (ISMAR-Adjunct)*, pages 5–12, 2020.
- [Nit17] V. Nityananda and J. C. A. Read. Stereopsis in animals: evolution, function and mechanisms. *The Journal of Experimental Biology*, 220(14):2502–2512, 2017.
- [Sch03] T. W. Schubert. The sense of presence in virtual environments: A three-component scale measuring spatial presence, involvement, and realness. *Zeitschrift für Medienpsychologie*, 15(2):69–71, 2003.
- [Sea00] A. Searle, K. Vedhara, P. Norman, A. Frost, and R. Harrad. Compliance with eye patching in children and its psychosocial effects: A qualitative application of protection motivation theory. *Psychology, Health & Medicine*, 5(1):43–54, 2000.
- [Sin12] H. Singh and J. Singh. Human eye tracking and related issues: A review. *International Journal of Scientific and Research Publications*, 2(9):1–9, 2012.
- [Ver15] V. J. M. Verhoeven, K. T. Wong, G. H. S. Buitendijk, A. Hofman, J. R. Vingerling, and C. C. W. Klaver. Visual consequences of refractive errors in the general population. *Ophthalmology*, 122(1):101–109, 2015.
- [War18] L. M. Ward, G. Morison, A. J. Simmers, and U. Shahani. Age-related changes in global motion coherence: Conflicting haemodynamic and perceptual responses. *Scientific Reports*, 8(1):1–11, 2018.
- [Wat94] J. Wattam-Bell. Coherence thresholds for discrimination of motion direction in infants. *Vision research*, 34(7):877–883, 1994.
- [Wat04] S. Watt, K. Elliott, M. Bradshaw, P. J. Simpson, I. Davies, and P. Hibbard. Binocular cues and the control of prehension. *Spatial vision*, 17(1-2):95–110, 2004.

- [Wri06] K. W. Wright, P. H. Spiegel, and L. S. Thompson. *Handbook of pediatric strabismus and amblyopia*. Springer Science+Business Media Inc, New York, 2 edition, 2006.
- [Žia17] P. Žiak, A. Holm, J. Halička, P. Mojžiš, and D. P. Piñero. Amblyopia treatment of adults with dichoptic training using the virtual reality oculus rift head mounted display: preliminary results. *BMC Ophthalmology*, 17(1):1–8, 2017.